Novel Therapeutic Approaches for Glioblastoma

by

Mostafa Khairy

A thesis submitted in partial fulfillment of the requirements for the degree of

Master of Science

Medical Sciences – Pediatrics

University of Alberta

Abstract

Glioblastoma has a devastating prognosis, and a remarkably low survival rate. Current therapeutic strategies including surgery, radiation and temozolomide are only useful as a palliative therapy, with no significant increase in overall survival. In this study, we investigated multiple therapeutic approaches, both as a new main treatment and as an adjuvant therapy to enhance the sensitivity of glioblastoma cells to radiation.

Histone acetylation and deacetylation is an important epigenetic mechanism for controlling gene expression and DNA repair. Histone acetylation and deacetylation are controlled by two classes of enzymes: Histone acetyltransferases (HATs) and Histone deacetylases (HDACs). Histone acetylation occurs on the lysine residues of histones, which neutralizes the lysine positive charge, leading to weakening of the electrostatic attraction between those residues and DNA. This induces a less condensed chromatin condition, which enhances the accessibility of DNA binding proteins to DNA. We postulated that the inhibition of histone acetylation will increase the sensitivity of glioblastoma cells to radiation. In the first part of my thesis, I used immunofluorescence microscopy to examine the effect of HAT inhibition on chromatin condensation and DNA double strand breaks after radiation, with no significant effect observed.

HATs use acetyl CoA as the substrate for histone acetylation. Acetyl CoA is produced in the cell through various metabolic pathways, which include glucose, fatty acids, and glutamine metabolism. It has been reported that the acetyl CoA that is used for histone acetylation comes mainly from glucose metabolism in a panel of colorectal, prostate, glioblastoma and breast cancer cell lines. In the second part of my thesis, I investigated the effect of glucose concentrations in culture media on histone H3 and histone H4 acetylation, with the goal of controlling histone

acetylation with glucose concentration and determining the impact on DNA repair. However, glucose concentration in the media had no effect histone acetylation.

Finally, in the third part of my thesis, I examined whether tumor selective energy deprivation using 'ketogenic diet' culture media might affect the growth of glioblastoma cells. Research from different labs showed that glioblastoma cells have impaired mitochondrial function, and less active OXCT1 3-oxoacid-CoA transferase 1, leaving them with a disrupted ability to metabolize a ketogenic diet. We saw this as a therapeutic window opportunity, with a ketogenic diet affecting energy production in glioblastoma cells but not affecting the normal cells in the brain. Our results indicated that both healthy tissue and glioblastoma cells were unable to use the ketogenic diet for energy production. Therefore, we did not pursue this approach.

Finally, in the last part of my thesis, I evaluated sulforaphane, a natural product that occurs in broccoli sprouts, as a new therapeutic approach for glioblastoma, for its anti-cancer properties. I found that sulforaphane exerted a cytotoxic effect on both U251 and U87 cells in a dose responsive manner. In addition, sulforaphane showed anti-invasion in U87 cells and cell cycle inhibition effects in U251 glioblastoma cells. Sulforaphane, however, did not enhance radiation cytotoxicity using the alamarBlue cytotoxicity assay. In conclusion, we believe that sulforaphane is a good candidate for in vivo studies and further research for glioblastoma therapy.

In conclusion, in this thesis we investigated different strategies to increase the efficacy of radiation treatment in glioblastoma therapy. The methods we used included HAT inhibition, changing the glucose concentration to affect histone acetylation, ketogenic diet media and sulforaphane. Among these, only sulforaphane showed cytotoxic, anti-invasive and cell cycle inhibition effects on glioblastoma cells. For future directions, we plan to test sulforaphane synergy with radiation.

Acknowledgements

I would like to thank my supervisor, **Dr. Sujata Persad**, who accepted me as a mentee in her lab, listened to my ideas, trusted my judgement, encouraged me to write a grant, supported me during my degree and cared for me at my lowest points. She has been a great support all along, and without her guidance, I wouldn't have been able to finish this degree. I want to thank my co-supervisor, **Dr. Roseline Godbout**, for the wisdom and knowledge she gave me, the great support in my scholarships and my applications, the encouragement and motivation for my future career prospects, for the faith she showed in my future successes, and for constantly offering all her resources to help me. I don't believe I would have been able to be where I am now without her support.

I would like to deeply thank **Dr. Michael Hendzel** for all his valuable insights. His guidance and mentorship during this degree were priceless. I owe most of my knowledge in this area of research to him. I remember the humbleness mixed with great motivation that I felt after all our meetings, which informed me that I have a lot to learn. I don't believe I would have been able to perform these experiments and design those ideas without his mentorship. And I hope to continue learning from him and getting more of his wisdom in my career.

I want to thank **Dr. David Eisenstat** for his valuable contributions and insights in our committee meetings, and for being a great mentor whom I have spent time in his lab with great welcome. In addition, I thank **Dr. Jerome Yager**, for the opportunity to collaborate with him on sulforaphane research and for being supportive along my path, and for teaching me a lot.

Thank you to the past and present members of the Persad and Godbout Labs, who helped and supported me, and taught me a lot: Ed, Elizabeth, Liz, Lei, Daniel, Jack, Xia, Zeenat and

Jocelyn. Special thanks to Hossein Doosti, my best friend, and the one who always supported, taught, listened to me, and guided me through all my hardships. A lot of thanks to the amazing people: Trish, Mikhaila and Sue, who help all the students.

Thanks to the technical assistance in this work, Ms. Geraldine Barron and Dr. Xuejun Sun from the Cell Imaging Facility, April at the radiation facility at the Cross Cancer Institute.

I would like to acknowledge and thank the awarding and funding agencies: Kids with Cancer Society, WCHRI, University of Alberta, Faculty of Medicine and Dentistry, and CRINA.

Special thanks to my amazing father and mother (Dr. Hossam and Dr. Abeer). If I were to choose the perfect parents, I wouldn't have been able to ask for more than them. Thank you for everything, I am here because of you. I want to thank my brother Marwan, my closest and best friend in this world, and whom I predict a great future for. Thanks to my great friends that never left my side all the time.

Finally, and most importantly, I thank God for everything, I am grateful for all his blessings, the ability to learn and understand and the strength to keep going. All this work and the upcoming work is for him.

Table of contents

Abstract ii

Acknowledgements iv

List of figures viii

List of abbreviations x

1.0 Introduction 2

Gliomas overview 2

1.1.1 Etiologies of gliomas 3

1.1.2 Genetic disruptions in glioblastoma 4

1.1.3 Epigenetic disruptions in glioblastoma 7

1.1.4 Therapeutic approaches 13

Protecting the DNA of normal cells 15

Sensitizing the glioblastoma cells to radiation by controlling DNA repair 16

Ketogenic diet 21

1.5 Sulforaphane 22

1.6 Rationale for the study 25

1.6.1 Hypotheses 26

1.6.2 Objectives 26

2.0 Materials and methods 28

2.1 Cell culture 28

2.2 Immunofluorescence 28

2.3 Semiquantitative PCR 29

2.4 Primers for Semiquantitative PCR 29

2.5 RT- qPCR 30

2.6 Primers for RT-qPCR 31

2.7 Histone extraction 31

2.8 Western blots 32

2.9 Assessment the effect of glucose on histone acetylation and the upregulation of histone acetylation after radiation 33

2.10 Testing the effect of glucose deprivation, on DNA repair 33

2.11 Sulforaphane 33

2.12 Sulforaphane treatment 34

2.13 alamarBlue cytotoxicity 34

2.14 Invasion Assay 34
2.15 Cell Cycle analysis with propidium iodide 35
2.16 Cell viability at different glucose concentrations 36
2.17 Cell viability in different concentrations of β-Hydroxy Butyrate 36
2.18 Cell viability in different concentrations of β-Hydroxy Butyrate with 2.5 mM glucose 36
2.19 Cell viability in different glucose concentrations with 5 mM β-Hydroxy Butyrate 37
2.20 Statistical Analysis 37
2.21 Imaging details 37
2.22 Foci quantification using Imaris 37
2.23 Table of antibodies 38
2.24 Table of inhibitors 39
2.25 Cell irradiation 39
3.0 Results 41
3.1 Sensitizing glioblastoma cells to radiation by manipulation of histone acetylation 41
3.1.1 Glioblastoma chromatin state compared to astrocytes 41
3.1.2 Semi quantitative and quantitative PCR for HAT genes 43
3.1.3 HAT inhibition's effect on the nuclear volume 45
3.1.4 HAT inhibition effect on the number of γH2AX foci after radiation. 46
3.1.5 The effect of glucose concentration in the medium on histone acetylation 49
3.1.6 Glioblastoma cell lines cannot survive without glucose 53
3.1.7 Glioblastoma cells did not survive when cultured in different β-Hydroxy Butyrate concentrations and no glucose media. 55
3.1.8 β-Hydroxy Butyrate showed no difference in survival upon adding 2.5 mM glucose 57
3.1.9 Cell viability curve with different glucose concentrations and 5 mM β-Hydroxy Butyrate. 59
3.2 Sulforaphane as an alternative therapy for glioblastoma. 61
3.2.1 Cytotoxic effect of sulforaphane on glioblastoma cell lines at a relatively low dose 61
3.2.2 Sulforaphane inhibited U87 invasion in a significantly low dose. 65
3.2.3 Sulforaphane caused U251 cell cycle arrest 66
4.0 Discussion 71
5.0 Conclusions and future directions 81
Bibliography 83

List of figures

Figure1: Rationale for using ketogenic diet in glioblastoma

Figure2: Sulforaphane mechanisms in glioblastoma

Figure3: Comparison of astrocytes and U87 nuclear volumes

Figure4: semiquantitative PCR for HAT genes

Figure5: Effect of HAT inhibition on nuclear volume

Figure6: Effect of different HAT inhibitors on γH2AX foci number.

Figure7: Western blot for histone acetylation

Figure8: Immunofluorescence for cells after radiation at different glucose concentrations

Figure9: Glioblastoma cell lines survival at different glucose concentrations

Figure10: Glioblastoma cells survivability at different β-Hydroxy Butyrate concentrations.

Figure11: Glioblastoma cells survivability at different β-Hydroxy Butyrate concentrations and 2.5 mM glucose.

Figure12: Cell viability curve with different glucose concentrations and 5 mM β-Hydroxy Butyrate.

Figure13: Sulforaphane cytotoxicity on U87 and U251 cell lines.

Figure14: Sulforaphane cytotoxicity on human astrocytes and fibroblasts cell lines.

Figure 15: Sulforaphane effect on invasion

Figure 16: Sulforaphane effect on cell cycle

Figure 17: Sulforaphane effect on histone acetylation

Figure 18: Sulforaphane synergy with radiation

List of abbreviations

ACLY: ATP citrate lyase

BRDs: Bromodomains

βHB: β-hydroxybutyrate

DAPI: 4′,6-Diamidino-2-phenylindoleDDR: DNA-damage response

DMEM: Dulbecco's modified eagle medium

Dnmt1: DNA methyltransferase 1

DSB: Double strand breaks

EGFR: Epidermal growth factor receptor

FBS: Fetal bovine serum

HATs: Histone acetyltransferases

H2A: Histone 2A

H2B: Histone 2B

H3: Histone H3

H4: Histone H4

HDACs: Histone deacetylases

HDR: Homology directed repair

LD50: Lethal dose to achieve 50% cell death

MGMT: O^6-methylguanine-DNA methyltransferase

NO: Nitric oxide

NHEJ: Non-homologous end joining

Nrf2: Nuclear factor E2-related factor

O_2^-: Superoxide

OGD: Oxygen and glucose deprivation

$ONOO^-$: Peroxynitrite

OXCT1: 3-Oxoacid-CoA transferase.

PBS: Phosphate buffer saline

PFA: Paraformaldehyde

PVDF: Polyvinylidenedifluoride

RB: Retinoblastoma

RIPA: Radioimmunoprecipitation assay

ROS: Reactive oxygen species

SFA: Sulforaphane

SOCS1: Suppressor of cytokine signaling 1 gene

TBS: Tris-base, NaCl

TBS-T: TBS and Tween

TMZ: Temozolomide

CHAPTER 1: Introduction

1.0 Introduction

Gliomas overview

The term 'glioma' includes all tumors that are of glial cell origin. Gliomas include astrocytic tumors which are classified by World Health Organization (WHO) as astrocytoma grades I, II, III and IV [glioblastoma][1]. Four malignancy grades are recognised by the WHO system, with grade I tumors the biologically least aggressive and grade IV the biologically most aggressive tumors[2]. Glioblastoma is the most common primary malignant brain tumor, comprising 16% of all primary brain and CNS neoplasms[3]. glioblastoma patients have a very bad prognosis, with a one-year survival rate of 37.2%, and a five-year survival rate of 5.1%[4]. The standard intervention for glioblastoma is maximal total resection followed by radiation and temozolomide[5]. Temozolomide is a DNA alkylating agent that was shown to significantly improve the survival rate when used in combination with radiotherapy[6]. Temozolomide methylates the DNA by adding methyl groups at N^7 and O^6 sites on guanines and the O^3 site on adenines in genomic DNA, which induces cell cycle arrest at G2/M and results in apoptosis[7]. Despite maximal initial resection and multimodality therapy, about 70% of glioblastoma patients will experience disease progression within one year of diagnosis, with less than 5% of patients surviving five years after diagnosis[5]. In a meta-analysis of 12 randomized clinical trials, the overall survival rate for patients with high-grade gliomas (e.g., glioblastomas and anaplastic astrocytomas) was 40% at 1 year and only slightly higher (46%) after combined radiotherapy and chemotherapy[8]. Additional radiation may be possible for some patients, but tolerance of healthy brain tissue to radiation is limited because of the increased risk of radiation necrosis[5]. Thus, limiting dosing of radiation or chemotherapy while maintaining anticancer efficacy is highly desirable.

Except for astrocytomas, there appears to be no hereditary component for gliomas. A population study that was conducted in northern Sweden showed that only familial astrocytoma occurred among first degree relatives, but not other histological types of brain tumors[9]. In agreement with the Swedish study, there was no statistically significant increase in glioma in relatives of glioma patients, in a study carried out on an Icelandic population[10].

Increased intracranial pressure or regional or general brain dysfunction are likely causes of an astrocytic tumor patient's symptom. Symptoms such as headaches, vomiting and papilloedema are caused by raised intracranial pressure[2]. As well, regional, or general brain dysfunction may lead to focal or general convulsions or alterations in consciousness. Other symptoms may include personality changes and mental deterioration[2]. Tumors in the cerebellum could lead to ataxia and often nystagmus along with symptoms of increased intracranial pressure. Brain stem tumors cause symptoms related to local infiltration with findings such as cranial nerve palsies, long-tract signs and ataxia[2].

1.1.1 Etiologies of gliomas

Some dietary components have been linked to glioma risk in adults. In experimental animals, intake of foods containing N-nitroso compounds were shown to be potent neuro-carcinogens. High intake of cured meat, cooked ham, processed pork and fried bacon, which contain elevated amounts of nitrite, was shown to be associated with a high risk for glioma[11–13]. Data from multiple animal studies suggest the possibility of neuro-carcinogenicity of endogenous and exogenous chemicals such as reactive oxygen species (ROS), N-nitroso compounds, and polycyclic aromatic hydrocarbons. However, in humans, glioma epidemiology studies have resulted in insignificant and inconsistent results[1].

Therapeutic or high-dose radiation is the only well established exogenous environmental cause of glioma. High dose chemotherapy for organs other than the brain has been also tied to gliomas[1]. The degree of risk from these exposures is dependent on genetic factors. For instance, it has been demonstrated that children with germline polymorphisms that result in low or absent thiopurine methyltransferase activity, are significantly more likely to develop brain cancer upon treatment with cranial irradiation and intensive anti metabolite therapy for acute lymphocytic leukemia[1]. Several genes were found to distinguish patients who developed brain tumors after those treatments from those who did not[14].

1.1.2 Genetic disruptions in glioblastoma

In the city of Zurich, Switzerland, which has a population of 1.16 million, a population-based study was conducted to find out the frequency of the major genetic disruptions in glioblastomas and their impact on patient survival. Amongst glioblastoma patients, the most common genetic disruption was loss of heterozygosity 10q (69%), followed by epidermal growth factor receptor (EGFR) gene amplification (34%), TP53 mutations (31%), p16INK4a deletion (31%), and PTEN mutations (24%). LOH 10q was associated with many of the other genetic disruptions and predicted a shorter survival. Primary (de novo) glioblastomas were the most prevalent (95%), while secondary glioblastomas that occurred through the progression of low-grade or anaplastic gliomas were rare (5%). Secondary glioblastomas were characterized by frequent loss of heterozygosity 10q (63%) and TP53 mutations (65%)[15].

One of the key mutations found in glioblastomas are those that happen in the Isocitrate dehydrogenases (IDH) 1 and 2 genes. Isocitrate dehydrogenases (IDH) 1 and 2 are important metabolic enzymes that reduce nicotinamide adenine dinucleotide phosphate (NADPH) to keep a

pool of reduced glutathione and peroxiredoxin, and form α-ketoglutarate, which is a co-factor for multiple enzymes. IDH1/2 is mutated in the majority of secondary glioblastoma and ~70–80% of lower-grade gliomas. The mutant IDH1 (R132H) not only loses its normal catalytic activity but also gains a new one which produces d-(R)-2-hydroxyglutarate (2-HG). The upregulation of 2-HG in cancer cells interferes with cellular metabolism and inhibits histone and DNA demethylases, This leads to DNA hypermethylation which in turn blocks cellular differentiation[16].

Genetic disruptions in glioblastoma have also been found at the EGFR gene, which encodes a receptor tyrosine kinase. Point mutations have resulted in a truncated EGFR protein, EGFRvIII, as the result of a frameshift mutation. EGFRvIII lacks 267 amino acids in the extracellular domains. These missing amino acids result in a constitutively activated receptor that no longer requires its ligand EGF to signal downstream[17]. Another EGFR disruption is the amplification of its gene, which occurs in 40-50% of glioblastomas[18]. When ligands bind to the extracellular domain of EGFR, it forms homo and heterodimers that phosphorylate the tyrosine residues in its intracellular domain, resulting in the activation of the receptor and conduction of a downstream signal. This receptor signals proliferation and survival of cells, therefore, its amplification can contribute to cancer formation[19].

Researchers studied the status of the CDKN2A, CDK4 and RB1 genes in gliomas. In one study of 120 glioblastoma samples, 40% showed loss or inactivation of the CDKN2A gene, 12% showed amplification of the CDK4 gene, and 14% showed loss or inactivation of the RBI gene. From these results, it can be surmised that most glioblastomas have genetic disruptions that lead to loss of control of the G1- S-phase transition of the cell cycle. The remaining glioblastomas (~30%) were missing one allele of the CDKN2A and/or RBI genes. Only 6% of the glioblastomas had no aberrations of these genes. Similar alterations were seen in anaplastic astrocytomas but at lower

frequencies, with 34% showing no disruptions of the analysed genes. The astrocytomas demonstrated loss of only one allele of the RBI gene in 28% of tumors, while retaining one wild-type copy[20].

Deregulation of the G_1-S transition during the cell cycle is one of the most important mechanisms for tumorigenesis. Therefore, the cell has multiple mechanisms in place to trigger apoptosis in cells that have lost cell cycle control. However, in glioblastoma, these endogenous safety mechanisms were found to be disrupted. As mentioned above, two-thirds of glioblastomas showed disruptions of G1-S transition control through amplification of *CDK4* or mutation/homozygous deletion of RB1 *or* CDKN2A *(*$p16^{INK4A}$*).* Normally, these deregulations of G_1-S transition control genes would stimulate p53-dependent apoptosis in cells. p53 prevents cells from uncontrolled proliferation and tumor formation by inducing either G_1 arrest or apoptosis. One mechanism for p53 activation is through $p14^{ARF}$. When $p14^{ARF}$ is activated as the result of abnormal cell cycle entry, it inhibits the degradation and silencing of p53 by MDM2, leading to p53 accumulation. In a study of gliomas, it was found that 76% of glioblastomas (103 of 136), 72% of anaplastic astrocytomas, and 67% of astrocytomas (10 of 15) had an inactivated p53 pathway either by mutation of *TP53* (uncommon), amplification of MDM2, or homozygous deletion/mutation of $p14^{ARF}$. Furthermore, it was shown that 96% of glioblastomas and 88% of anaplastic astrocytomas with abnormal G_1-S transition control also had a deregulated p53 pathway. Thus, it appears that cell cycle disruption is almost always coupled by p53 pathway aberration, which indicates the importance of p53 as a safety mechanism against tumorigenesis[21].

Another mechanism for p53 pathway inactivation comes from the microenvironment of glioblastoma. In vivo, glioblastomas grow in a hypoxic and inflammatory microenvironment, where there are upregulated levels of the free radicals, nitric oxide (NO) and superoxide (O_2^-). Out

of these increased levels of NO and O_2^-, peroxynitrite ($ONOO^-$) can arise. The latter is a highly reactive molecule that can post-translationally modify and inactivate proteins, especially zinc finger transcription factors such as p53. It was shown that glioblastomas demonstrate tyrosine nitration, which is evidence of protein modification by peroxynitrite *in vivo*. In glioma cells, peroxynitrite inhibits both the function and the specific DNA binding ability of wild type p53 protein. Furthermore, concentrations of peroxynitrite associated with a tumor inflammatory environment caused dysregulation of wild-type p53 transcriptional activity and downstream $p21^{WAF1}$ expression[22]. This could explain the consistent deactivation of the p53 pathway observed in gliomas, despite the lack of mutations in the gene itself.

1.1.3 Epigenetic disruptions in glioblastoma

Other than genetic disruptions, glioblastomas are also characterized by major epigenetic disruptions.

1.1.3.1 Genome hypomethylation

In many cancers, genome hypomethylation is a main feature that is thought to contribute to tumorigenesis independently from the hypermethylation of CpG island[23]. Induced hypomethylation in mice containing a hypomorphic allele of DNA methyltransferase 1 (Dnmt1), which leads to broad hypomethylation in all tissues, resulted in an aggressive T-cell lymphoma with a common chromosome 15 trisomy[24]. This indicates that hypomethylation plays a significant role in tumorigenesis[24]. This tumorigenesis may be due to several mechanisms that were demonstrated in different studies. (i) Hypomethylation may cause chromosomal instability, which has been associated with different types of cancers such as sarcoma and prostate cancer[24–26]. (ii)

DNA methylation can suppress transposable elements, with hypomethylation shown to activate endogenous retroviral element insertions, which may activate proto-oncogenes, leading to tumorigenesis[24,27]. (iii) Hypomethylation can alter gene expression in glioblastoma leading to activation of proto-oncogenes[24,28].

In glioblastoma, hypomethylation occurs at high frequency in both tissues and cell lines. However, not all glioblastoma primary tumors show genomic hypomethylation, indicating that these tumors can develop without hypomethylation. An example of genome hypomethylation effects in glioblastoma is a study showing a trend between global DNA methylation levels and the methylation status of the juxta-centromeric SAT2 DNA repeat region. This study showed that in two glioblastoma primary tumors, severe Sat2 hypomethylation was associated with gene copy number alterations with breaks that appeared precisely next to the centromere adjacent region of Chr1p. In contrast, glioblastomas characterized by mild Sat2 hypomethylation had normal gene copy numbers. A Chr1q copy gain was found in glioblastoma with a 1q12 breakpoint, and that copy gain correlated with Sat2 hypomethylation. On the other hand, D4Z4 repeat hypomethylation occurred to a lesser extent in globally hypomethylated glioblastoma and led to altered gene expression rather than chromosomal instability. Demethylation of CpG sites in the MAGEA1 promoter correlates with its expression levels. In glioblastoma, demethylation correlated with MAGEA1 expression levels, indicating that methylation was a silencing mechanism for this gene in the brain[29].

1.1.3.2 Hypermethylation

Gene promoter hypermethylation was first reported to be associated with gene expression in 1986, when two researchers at Johns Hopkins noticed that site specific hypermethylation of Calcitonin was associated with its silencing. After that, this phenomenon was observed with the first known

tumor suppressor gene, the retinoblastoma gene RB, which led to the conclusion that genetic hypermethylation is a direct mechanism for tumor-suppressor gene silencing[30]. In glioblastoma, promoter hypermethylation is associated with important tumor suppressor genes that are involved in key cellular processes including cell cycle regulation, DNA repair and apoptosis such as Tp53, PTEN and retinoblastoma (RB) genes[31–33].

Moreover, promoter hypermethylation may be involved in invasion and drug resistance. For example, hypermethylation was involved in silencing of the Protocadherin family member PCDH-γ-All in astrocytomas, which is thought to be associated with the invasion of tumor cells into brain parenchyma[34]. In addition, the suppressor of cytokine signaling 1 gene (SOCS1) was found to be silenced in ten different glioblastoma cell lines, and the restoration of its expression sensitized the glioblastoma cell lines to ionizing radiation[35].

One important example of hypermethylation in glioblastoma is the O^6-methylguanine-DNA methyltransferase (MGMT) promoter hypermethylation. The MGMT gene codes for the MGMT enzyme which is involved in DNA repair by removing alkyl adducts from the guanine and thymine[36]. However, in tumor cells, this function makes this enzyme the major mediator in glioblastoma resistance to alkylating agents. Therefore, MGMT silencing by promoter methylation increases the sensitivity of cancer cells to temozolomide chemotherapy, thus making MGMT promoter methylation status an important prognostic marker for glioblastoma response to temozolomide. It was observed that elderly patients (>65–70 years) with glioblastoma tumors lacking MGMT promoter methylation get minimal effect from such therapy, underlying the importance of testing the MGMT promoter methylation status in neuro-oncology[37].

Based on CpG islands methylation status, researchers attempted to classify glioblastoma into different subtypes, to explain the heterogeneity in treatment response and prognosis and provide a guide for clinicians to choose the treatment protocol. Previously, glioblastomas were classified based on their transcriptional fingerprints into four subtypes: classical, neural, proneural, and mesenchymal. However, this classification included in the analysis the transcriptomes of non-malignant cells associated with the tumor[38]. Newer classifications have since been generated, one of which has proven to be very important clinically. This latter classification is based on the methylation status of the tumor and makes use of an unsupervised machine learning algorithm to classify glioblastomas according to their methylation status. An online tool was then created, allowing doctors to upload methylation data and obtain methylation-based classification of the glioblastoma. This classification was shown to be very reliable in making therapeutic decisions[39]. Other studies also came up with classifications based on methylation data. In one study, three glioblastoma molecular subtypes were identified by consensus clustering of the methylation profiles of 11,637 CpG sites that significantly correlated with survival. These three subtypes showed different survival curves from each other[40]. Another study assessed the global methylation of long interspersed nuclear elements-1 (LINE1) in 12 candidate genes, and then by unsupervised clustering analysis, three methylation patterns were designated to three different classes. In the first class, promoters from the following genes, MGMT, PTEN, RASSF1A, TMS1, ZNF342, EMP3, SOCS1, and RFX1 were highly methylated in 82% (75/91) of lower-grade astrocytic and oligodendroglial tumors, 73% (8/11) of secondary glioblastoma, and 12% (6/52) of primary glioblastoma. In the second class, HOXA9 and SLIT2 were highly methylated in 37% (19/52) of primary glioblastoma. None of those 10 genes were methylated in class 3. These different classes were correlated with gene expression of EZH2 and IGFBP2 and the patient survival times[41]. These

studies suggest that hypermethylation patterns could be beneficial as a classification system to be correlated to patient prognosis and treatment recommendations.

1.1.3.3 Histone modifications

One of the most important factors affecting DNA replication, transcription, repair, and recombination is the chromatin constitution. The chromatin consists of a combination of DNA and histones in a structural unit that is called the nucleosome. The nucleosome consists of a 147 base pairs , wrapped twice around a disc-shaped octamer composed of two copies of each histone protein (H2A, H2B, H3, and H4)[42]. These core histones can be reversibly modified by different types of chemical modifications such as methylation, phosphorylation, acetylation, ADP ribosylation, sumoylation, ubiquitylation and deamination. These modifications can be found in two parts in the histone proteins, either in the amino acids constituting the core or the amino-terminal tails, where they play essential structural and functional roles in maintaining the dynamic equilibrium between chromatin and gene regulation[43]. Of all these modifications, histone acetylation and methylation are the most studied. In this thesis, we focused on histone acetylation only.

Histone acetylation and deacetylation is an important mechanism for controlling gene expression in cells. The acetylation pattern of different promoters is controlled by two major classes of enzymes: histone acetyltransferases (HATs), and histone deacetylases (HDACs). Histone acetyltransferases catalyze the acetylation of lysine residues on the tails of histones that comprise the nucleosomes of the chromatin. Acetylation of these residues neutralizes the positive charge on the lysine which reduces the affinity between the DNA and acetylated histone residues. This process results in loosening of the chromatin, enhancing the accessibility of transcription factors to the DNA[18].

Another extensively studied modification is histone methylation, which is a covalent post-translational modification that occurs on the side chain nitrogen atoms of lysines and arginines. Arginine can be either mono- or di-methylated, and the reaction is catalyzed by Protein arginine methyltransferases (PRMTs). Lysine methylation can also occur in mono-, di-, and tri-methylated forms. Depending upon the lysine, methylation can be a marker of transcriptionally active euchromatin or transcriptionally repressed heterochromatin[42]. Methylated lysines can be bound by a variety of domains, including Tudor, chromo, PWWP, MBT and PHD. Histone methylation enhances the binding affinity of the chromodomains of HP1 and Polycomb. This effect of increasing the affinity of histone tails for certain proteins appears to enhance nucleosome stability[44]. Thus, alteration of histone modifications is linked to changes in gene expression, and was shown to manifest in many cancers[45].

Global deviation at the histone level occurs because of mutations in genes coding for regulatory enzymes, including HDACs (HDAC2 and HDAC9), histone demethylases (JMJD1A and JMJD1B), and histone methyltransferases (SET7, SETD7, MLL3, and MLL4), as observed by a large-scale genomic analysis of glioblastoma samples[42]. In addition, class II and IV HDACs mRNA levels were found to be downregulated in glioblastomas in comparison to low-grade astrocytomas[46]. Moreover, it was observed that histone H3 (but not histone H4) was more acetylated in glioblastomas than normal brain tissue [46].

In addition, mutations in the genes encoding the histone proteins themselves, can result in changes in the modification sites. For instance, it was found that 78% of pediatric diffuse intrinsic pontine glioma (DIPG) and 22% of non-brainstem pediatric glioblastomas (non-BS-PGs) had a mutation in H3F3A, that encodes histone H3.3, or in the related HIST1H3B, that encodes histone H3.1,

resulting in a Lys27Met amino acid replacement in each protein. Furthermore, another 14% of non-BS-PGs contained somatic mutations in H3F3A causing a p.Gly34Arg substitution[47,48]. These H3F3A mutations were also found by the Jabado lab to be present in 31% of the tumor samples analyzed, and they led to amino acid alteration at two key regulatory post-translational modification positions within the histone tail (K27M, G34R/G34V)[49].

1.1.4 Therapeutic approaches

There are not many therapeutic approaches that are clinically effective in glioblastoma. As mentioned earlier, the standard treatment for glioblastoma is surgical removal, followed by radiation and temozolomide[5]. Some patients might need additional radiation, but tolerance of healthy brain tissue to radiation is limited because of necrosis caused by radiation[5].

Temozolomide is a DNA alkylating agent that was shown to significantly improve the survival rate when used in combination with radiotherapy[6]. However, the median increase in survival is only 2.5 months[50,51]. In addition, trials have shown a lack of efficacy of temozolomide in pediatric glioblastoma[52]. Methylation of the MGMT (O-6-Methylguanine-DNA Methyltransferase) promoter does however potentiate the efficacy of temozolomide, even in children[53], and represents an important prognostic tool in glioblastoma therapy. The reason for this is that MGMT removes the alkyl adducts added by temozolomide. Therefore, methylation of its promoter leads to silencing of the gene, thus preventing MGMT protein production, which abolishes the protection mechanism against Temozolomide. However, glioblastoma has been shown to be resistant to radiation and chemotherapy through multiple mechanisms, including presence of glioblastoma stem cells, metabolic alterations, tumor microenvironment, tumor heterogeneity, hypoxia, microRNAs, and alteration in cell cycle regulation and DNA damage repair[54].

In addition to resistance mechanisms, the blood-brain barrier (BBB), which is the protective barrier of the central nervous system, makes it difficult to deliver certain drugs to the brain parenchyma which limits the sensitivity of brain tumors to the therapeutic effects of these drugs. The structure and function of the BBB changes with the progress of the tumor, with disruption of the BBB leading to better access of the drugs to the brain. Almost all macromolecular drugs such as monoclonal antibodies and about 98% of small molecules cannot infiltrate the central nervous system to exert therapeutic effects until late in cancer progression, which results in the failure of many drugs in clinical trials[55].

Most tumors grow rapidly, which leads to them outgrowing the blood vessels. This prevents the homogenous diffusion of oxygen to the entire tumor tissue which results in hypoxia. Glioblastoma tumors are no exception to this scenario, as they also contain hypoxic regions detected by MRI and microscopic analysis. Furthermore, it was shown that hypoxia-inducible factors (HIFs) make essential contributions to GBM tumorigenesis by regulating the tumorigenic capacity of glioblastoma stem cells. HIF2-α is activated by hypoxia, and then it activates OCT4, a stem cell transcription factor. Since OCT4 regulates the self-renewal and differentiation of stem cells, this leads to increasing stemness in glioblastoma cell populations[54].

Hypoxia also contributes to radioresistance in glioblastoma tumors. It has been shown that oxygen concentration affects the response of mammalian cells to radiation through different mechanisms. Firstly, the stemness of glioblastoma cell populations increases radioresistance. Moreover, the free radicals that induce oxidative stress, which is generated by radiotherapy, decreases under hypoxic conditions. This is supported by the observation that enhancing the tumor oxygenation increases glioblastoma radiosensitivity in vitro and in vivo[54].

Due to the extremely high recurrence rate of glioblastoma after the first line treatment, new therapies have emerged as a second line, which includes repeating the surgical resection, reirradiation, nitrosoureas, bevacizumab, a recombinant humanized monoclonal antibody which works by preventing angiogenesis through inhibition of vascular endothelial growth factor A (VEGF-A), or tyrosine kinase inhibitors[52,56–60]. However, none of these treatments have translated to increases in survival. Immunotherapy which has shown highly improved survival rates in other cancers, was thought to be promising in glioblastoma; however, results to date suggest that glioblastoma is a cold tumor.[7]. Tumors are categorised according to the tumor microenvironment into hot and cold tumors. Cold tumors are tumors that contain few if any infiltrating T cells. On the contrary, hot tumors contain many infiltrating T-cells in their microenvironment, which makes them responsive to immunotherapy[61].

Therefore, there is an urgent need to investigate new therapies for glioblastoma. To tackle this problem, we tried multiple new approaches to induce cytotoxicity and sensitize the glioblastoma cells to radiation. I will now discuss the background and rationale for each of the approaches investigated.

Protecting the DNA of normal cells

The goal of our first approach was to protect the DNA in normal cells from radiation, while maintaining its cytotoxic effect in glioblastoma cells. Based on the DNA superstructural effects of acetylation, we hypothesized that we could control the response to radiation as detailed here. As mentioned earlier, histone acetylation and deacetylation are an important mechanism for controlling gene expression in cells. The acetylation pattern of different promoters is controlled by two major classes of enzymes: histone acetyltransferases (HAT), and histone deacetylases

(HDAC). Histone acetyltransferases catalyze the acetylation of lysine residues on the tails of histones that comprise the nucleosomes on the DNA. Acetylation of these residues neutralizes the positive charge on the lysine which reduces the affinity between the DNA and acetylated histone residues. This process results in loosening the chromatin, which enhances the accessibility of transcription factors to the DNA[44]. Thus, inhibition of this process will result in tightly packed DNA which will be less accessible to the DNA damaging chemotherapy/radiation, therefore, conferring a protective mechanism on the DNA. However, in glioblastoma, because of their high requirement for replication, the cancer cells will counter HAT's inhibition by upregulation of HAT expression. The result of this would be that in the presence of HAT inhibition, glioblastoma cells will be more susceptible to DNA damage with radiation therapy than the neighboring normal cells. To test this hypothesis, I controlled the histone acetylation profile by inhibiting histone acetyltransferases and examined the radiation dosage boundaries for both glioblastoma cells and normal glial cells. The idea behind our hypothesis is that glioblastoma cells would resist HAT inhibition due to the demand for transcriptional availability in these very proliferative cells, making them susceptible to radiation.

Sensitizing the glioblastoma cells to radiation by controlling DNA repair

I also investigated whether glioblastoma can be sensitized to radiation by modifying/affecting DNA repair. As the number of double strand breaks (DSB) caused by radiation correlates with cell death[62], targeting DNA repair in cancer cells can sensitize cancer cells to radiation. Importantly, DNA repair should be differentially inhibited in cancer cells vs normal cells to obtain a therapeutic window. There are 3 potentially important features in tumors that make them more vulnerable to RT: (1) Tumors are under constant replicative stress that causes ongoing DNA double strand

breaks making them more dependent on DNA repair pathways than normal cells. (2) Many tumors have compromised DNA repair ability which increases their susceptibility to radiation compared to normal cells. (3) Many tumor cells are defective in cell cycle checkpoints, which contributes to their tumorigenesis, but also decreases their window of opportunity for DNA repair[63].

Ionizing radiation causes DNA double strand breaks (DSB), which activates one of two major DNA repair systems determined by the stage of the cell cycle at the time of the break: non-homologous end joining (NHEJ), and homologous directed repair (HDR)[64]. The primary pathway for repairing non-replication-associated breaks is NHEJ and it is the predominant pathway during cell cycle. On the other hand, HDR is not active at G1 and is activated mainly during late S–G2 phase. And, while in NHEJ, DSB ends are simply joined, HDR uses a sister chromatid as a template for repair[64]. In NHEJ, damaged DNA ends are detected by the Ku70/80 complex and DNA-PKcs, which leads to recruitment of nucleases that minimally process the damaged ends then catalyze re-ligation by DNA ligase IV, which is why NHEJ has low fidelity and can create mutations/deletions/insertions at the site of damage[65,66]. HDR requires end-resection of the DNA to produce a single-stranded (ssDNA) molecule, which then invades the sister chromatid to locate homologous DNA sequences that can prime repair. Thus, HDR is a high-fidelity repair mechanism[65,66]. However, DSB repair includes more than just rejoining broken regions of DNA. DSBs leads to the activation of a complex signaling cascade that is called DNA-damage response (DDR). This cascade is responsible for sensing the DNA damage, then the amplification and transmission of a damage signal to induce a multitude of cellular actions. DSBs are recognized by the MRE11-RAD50-NBS1 (MRN) complex, which recruits the ATM kinase to DSBs and induces ATM's kinase activity that results in phosphorylating the histone variant H2AX[67]. MDC1 then

binds to phosphorylated H2AX (γH2AX)[68], creating a platform for activated ATM, which enhances spreading of H2AX phosphorylation for hundreds of kilobase pairs along the chromatin[6]. In addition, MDC1 recruits the ubiquitin-ligases RNF8 and RNF168. Those ubiquitin-ligases are able to ubiquitinate both chromatin and histones H2A[69], which is required for recruitment of 53BP1, a dual reader that interacts with ubiquitinated H2AK13/15 (caused by RNF168) and H4K20me2 and its recruitment is essential for directing DSBs to either NHEJ or HDR repair choice[70].

The higher-order organization of chromatin is important in assembling the repair machinery, as it is essential for the accessibility of DNA lesions to the repair complexes, and might influence how readily a lesion is detected and repaired[64]. The basic unit of chromatin is called the nucleosome, and it is composed of two copies of each of the four core histones: H2A, H2B, H3 and H4, along with ∼147 bp of DNA wrapped around the histone core[71]. Histones have a common structure, with the central histone-fold region forming the core of the nucleosome, and N- and C-terminal tails that extend outwards from this core. The N-terminal tails of histones contain lysine residues that can have multiple modification groups at their ε-amino group[72,73]. Here we focus on one of these modifications that is significant for our proposal, which is Lysine acetylation. Lysine acetylation is carried out by a family of Lysine acetyltransferases (KATs) which transfer the acetyl group from acetyl-CoA to the ε-amino of lysine, causing neutralization of the positive charge on lysine[74]. In multiple studies, lysine acetylation in general was found to disrupt the electrostatic interactions between the histones and the phosphate groups in the DNA, leading to a looser chromatin configuration[75]. As well, acetylation of specific lysine residues was also observed to have a significant role in a looser chromatin configuration. For instance, acetylation at H4K16 inhibits

interaction between the H4 tail and a regulatory domain on the surface of the nucleosome called the acidic patch[76]. The acidic patch is formed by a concentration of acidic residues from histone H2A and histone H2B forming a shallow, acidic groove on the nucleosome's surface to which the unacetylated H4 tail can bind, promoting the formation of packed nucleosome arrays[77]. Therefore, blocking this interaction by acetylation of H4 (at lysine 16) leads to an open chromatin configuration that favors repair.

The role of acetylation is not only confined to the induction of open chromatin configuration but is also important for blocking other modifications on lysine residues, which is a mechanism for blocking the signal induced by those other modifications. An important example of this is the acetylation of H4K16 and H2AK15 by Tip60, which blocks the ubiquitination of H2A at K15. This acetylation blocks the binding of 53BP1 to the adjacent H4K20me2 and the H2Ak15 ubiquitin site[78,79]. 53BP1 binding directs the repair choice towards NHEJ, therefore, blocking its binding promotes HDR repair system[78,79]. Hence, lysine acetylation directly affects the choice of repair system in the DSB repair process. Finally, acetylation of histones also creates binding sites for a large family of chromatin proteins that contain bromodomains (BRDs)[80]. Those BRDs participate in diverse processes in DNA damage response, such as chromatin remodeling, transcriptional regulation and recruiting other complexes to the DSBs[80].

Histone acetylation requires acetyl CoA in the nucleus and is correlated with the availability of Acetyl CoA produced by the ATP citrate lyase (ACLY) enzyme acting on the citrate metabolite[81]. Further, glucose is the primary source for citrate production, and therefore is an important factor in determination the level of histone acetylation[82–88]. Normally, under glucose deprivation

conditions, cells can use fatty acid oxidation to support their bioenergetic needs. However, only mitochondrial acetyl CoA is produced from fatty acid oxidation, and not nucleocytoplasmic acetyl-CoA. Therefore, providing glucose-starved cells with fatty acids did not result in rescued histone acetylation, consistent with the model that only nucleocytoplasmic acetyl-CoA participates in histone acetylation[81]. Moreover, a mechanism for crosstalk between metabolic and DNA repair pathways was reported to be mediated by ACLY. Following DNA damage, nuclear ACLY is phosphorylated at S455 by ATM and AKT. ACLY phosphorylation and nuclear localization were observed to be essential for promoting BRCA1 recruitment and impairing 53BP1 localization, which enhances DNA repair by homologous recombination[89]. Based on this literature, it was speculated that changing glucose concentration would influence DNA repair. This was demonstrated in a hypopharyngeal carcinoma cell line (FaDu) and an adenocarcinoma human alveolar basal epithelial cell line (A549). In this study, glucose deprivation impaired DNA repair after ionizing radiation in the tumor cells but not the normal fibroblasts[90]. However, a recent report found that the availability of lipids could reprogram metabolism to become a major carbon source for histone acetylation[91].

Based on the above facts, I proposed that it is possible that glucose deprivation, by limiting substrate availability for acetylation and hence compromising DSB repair, will increase susceptibility of glioblastoma to radiation. Therefore, combining glucose deprivation with radiation may result in a decreased dosing requirement for radiation. We propose that glioblastoma cells, due to their high dependence on glucose/carbohydrates, are more susceptible to DNA damaging therapies than normal cells in the presence of histone acetylation inhibition through glucose deprivation.

Ketogenic diet

A ketogenic diet is a high-fat and low-carbohydrate diet that has been the subject of research interest for glioblastoma clinical trials[92]. Like other tumors, glioblastoma cells are characterized by high rates of glycolysis and lactate production (the Warburg effect). High rates of glycolysis and lactate production have also been observed in orthotopic mouse glioblastoma models. In mouse models of glioblastoma, tumor growth was reduced when a calorie-restricted ketogenic diet was applied. Furthermore, treatment of glioblastoma patients with a total meal replacement program with a ketogenic diet was well tolerated and suggested some antitumor activity[92]. The rationale behind using a ketogenic diet comes from the metabolic pathway for ketone bodies in the cell. Acetoacetate and 3-hydroxybutyrate are synthesized in the liver from acetyl-CoA that results from the beta-oxidation of fatty acids. Ketone bodies enter the citric acid cycle directly, bypassing cytoplasmic glycolysis. Glioblastomas have: (1) impaired mitochondrial function and (2) less active OXCT1 3-oxoacid-CoA transferase. Therefore, a ketogenic diet would induce tumor-selective energy deprivation[93]. Multiple reports demonstrated that a ketogenic diet supresses tumor growth and increases the radiation and chemotherapy efficacy in animal models[94]. Other reports showed that ketones such as β-hydroxybutyrate (βHB) can also inhibit cell growth and potentiate the effects of chemotherapy and radiation[95]. Therefore, we aimed to test the ability of both normal and cancer cells to survive using β-Hydroxy Butyrate, under no glucose conditions.

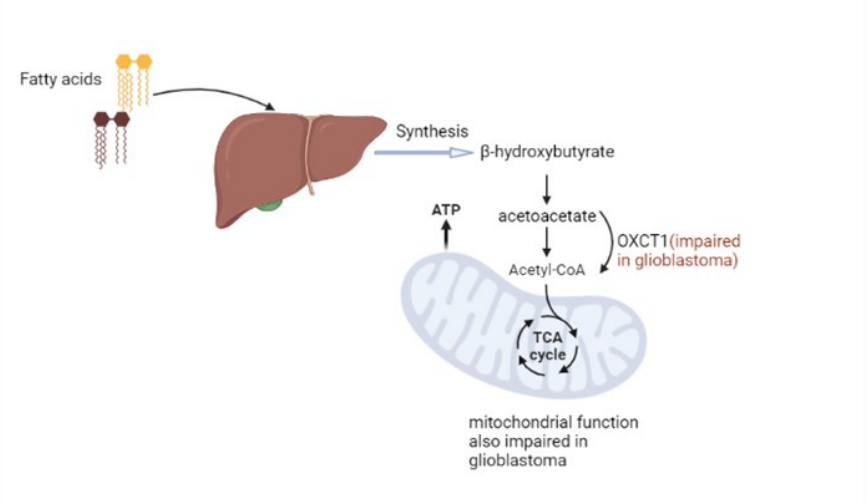

Figure1. Ketone bodies (acetoacetate and β-hydroxybutyrate) are produced in the liver through β-oxidation of fatty acids. Ketone bodies are metabolized in the cells by OXCT1 (3-oxoacid-CoA transferase) into acetyl CoA which then enters the citric acid cycle in the mitochondria. Glioblastoma has both impaired OXCT1 and mitochondrial activity, which disrupts the metabolism of ketone bodies. The figure was created using BioRender.

1.5 Sulforaphane

Isothiocyanate, 4-methylsulfinylbutyl, is commonly known as Sulforaphane (SFA), a compound that comes from the vegetables of the family Cruciferae, mainly, broccoli sprouts[96]. SFA is the product of the enzyme myrosinase acting on glucoraphanin, which results in the production of SFA by hydrolysis[97]. Both components exist in the broccoli sprout plant.

There is significant evidence supporting a neuroprotective role for SFA, which requires an anti-apoptotic and anti-necrotic activity[98]. However, surprisingly in cancer cells, SFA has been shown to promote apoptosis of cancer cells[99]. With that said, questions need to be addressed about the contradictory effects of Sulforaphane in normal cells versus cancer cells. Thus, several studies were conducted to investigate the mechanisms of SFA anti-cancer activity and determine the dosage needed to promote such an effect[99]. It appears that the mechanisms at the forefront of the SFA protective mechanism are significantly different than those utilized when SFA is active as an

anti-cancer agent. Interestingly, our data indicated that compared to the neuroprotective concentrations of SFA shown in our astrocyte cell cultures, 10X the concentration is required to cause glioblastoma cell death[96]. Here we demonstrate those mechanisms briefly with highlighting some of earlier research on Sulforaphane and glioblastoma.

One of the most common mechanisms in exerting anticancer activity is the generation of reactive oxygen species (ROS). Those are chemically reactive groups that contain oxygen such as peroxides and superoxides. In normal cells, ROS act as signaling molecules, but they are found to be elevated in almost all cancers due to the high metabolic activity of cancer cells[100]. This elevation leads to an intracellular toxic environment, causing cancer cells to upregulate the levels of antioxidant proteins, to counteract the oxidative stress. Therefore, if a certain compound increases the ROS in cancer cells to the extent that exceeds the capacity of antioxidant proteins, it will promote apoptosis and therefore exert anticancer effect. This was demonstrated upon addition of SFA to T24, a human bladder cancer cell line. ROS production was reported to be an early event upon the addition of SFA[101]. In addition, ROS production was also observed upon treatment of p53 deficient colon cancer cells with SFA. In both cases, these events induced by SFA resulted in apoptosis[102].

Epigenetic changes in cancer cells are one of the widely established mechanisms that results in changes in gene expression and leads to uncontrolled cell growth[103]. As mentioned earlier, one of the main epigenetic mechanisms is the change in histone acetylation and deacetylation status, controlled by histone acetyltransferases (HAT), and histone deacetylases (HDAC). These epigenetic changes in cancer cells could silence tumor suppressor genes and/or activate oncogenes. Thus, HDAC inhibitors were found to have an anticancer effect in many cancers, with different mechanisms, such as silencing oncogenes or stimulating tumor suppressor genes[104]. SFA was first

found to be a strong HDAC inhibitor in colorectal cancer cells[105]. Multiple studies then followed, demonstrating the same mechanism of SFA in other cancers[106]. For example, SFA addition inhibited HDAC6 in triple negative breast cancer cell lines. This inhibition of HDAC6 by SFA led to autophagy, and eventually cell death[107].

The MAPK/ERK pathway is a cascade of proteins in the cell that transfers a signal from a receptor on the cell surface to the DNA. In prostate cancer cell lines, SFA metabolites led to the phosphorylation of ERK1/2 which affected the downstream effectors, resulting in microtubule disruption and apoptosis[108]. The same pathway was found to be stimulated by SFA in non-small cell lung cancer, which also promoted apoptosis and anticancer effect[109].

Tumor suppressor genes stimulate cell cycle arrest and apoptosis. Therefore, they can exert an anticancer effect upon activation. Some examples of tumor suppressor genes include p53, p21, p27, and p73. SFA was observed to stimulate both p53 and p27, and suppress both cyclin-D1 and cMyc expression (oncogenes) in ovarian cancer cells, which resulted in their apoptosis[110]. In the MCF7 breast cancer cell line, SFA upregulated p53 and p21, resulting in G2/M cell cycle arrest[111]. Finally, in Xuanwei lung cancer cells, SFA increased p73 protein expression, leading to the upregulation of Bax (an apoptotic protein). This elevation of p73 resulted in the translocation of Bax to the mitochondria, activating the intrinsic apoptotic signaling pathway, leading to apoptosis[112].

1.5.1 SFA in glioblastoma

In glioblastoma, SFA was shown to act through different mechanisms. Firstly, by activating the ERK pathway. The MAPK/ERK pathway is a signalling pathway from the cell surface to the DNA. This pathway was stimulated in glioblastoma cell lines by SFA metabolite SFA N-acetyl cysteine

(SFA-NAC) and resulted in excessive autophagy that led to the disruption of alpha-tubulin and eventually autophagic cell death. Using the ERK inhibitor PD98059 reversed the effect of SFA-NAC[113]. SFA inhibited invasion via the same pathway, as well as regulation of downstream invasion-related markers, MMP-2 and CD44v6[114]. In addition, SFA elevated mitochondrial ROS levels in glioblastoma, which triggered ROS dependent cell death[115]. Furthermore, SFA was effective in eliminating glioblastoma stem cells[115]. Finally, SFA was shown to sensitize glioblastoma cells to temozolomide (TMZ) through the inhibition of the Wnt/β-catenin/TCF4 pathway. This led to the down-regulation of miR-21, which promoted the pro-apoptotic efficacy of TMZ in glioblastoma cells[116].

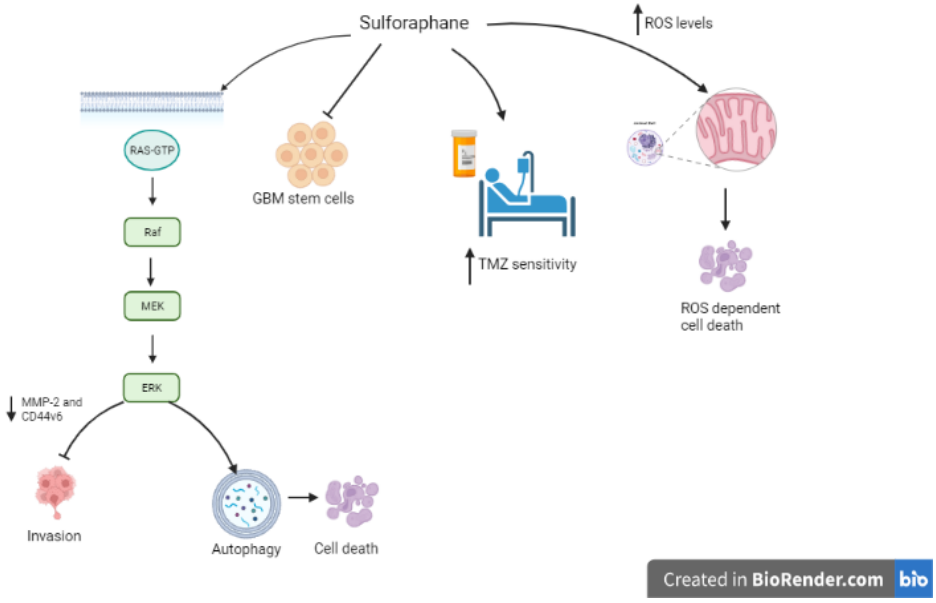

Figure2. Sulforaphane mechanisms in glioblastoma. Sulforaphane activated ERK pathway, which led to inhibition of invasion, autophagy and autophagic cell death. Sulforaphane eliminated glioblastoma stem cells. Moreover, it induced ROS elevation in the mitochondria, leading to cell death. Finally, it increases glioblastoma sensitivity to TMZ. The figure was generated using BioRender.

1.6 Rationale for the study

As seen from the research reviewed above, glioblastoma is a terminal illness with no current effective therapeutic strategies. Therefore, we aim to use different therapeutic strategies that were detailed earlier, to enhance the glioblastoma therapy.

1.6.1 Hypotheses

- HAT inhibition will cause a differential therapeutic response between glioblastoma cells and normal brain cells upon treatment with ionizing radiation, by protecting normal cells through chromatin condensation.
- Controlling glucose concentrations in the media would enable us to control histone acetylation, and therefore, exert an effect on DNA repair.
- Ketogenic diet would be metabolized by normal cells but not by cancer cells, which would exert a selective energy deprivation on glioblastoma cells
- Sulforaphane will exert an anti-cancer effect on glioblastoma cells and increase their sensitivity to radiation.

1.6.2 Objectives

- Control the histone acetylation either by HAT inhibition or glucose concentration and use this strategy to sensitize glioblastoma cells to radiation.
- Use ketogenic diet as an adjuvant therapy for glioblastoma.
- Assess the efficacy of SFA as an alternative treatment to glioblastoma.

CHAPTER 2: Materials and methods.

2.0 Materials and methods

2.1 Cell culture

U251 and U87 cell lines were obtained from Dr. Roseline Godbout's and Dr. David Eisenstat's labs and maintained in DMEM media supplemented with 10% FBS, 5% CO_2 and 1% Penicillin/Streptomycin antibiotic. Human astrocytes were bought from ScienCell and maintained in Human Astrocyte medium, consisting of 500 ml of basal medium, 10 ml of fetal bovine serum (FBS, Cat. No. 0010), 5 ml of astrocyte growth supplement (AGS, Cat. No. 1852) and 5 ml of penicillin/streptomycin solution (P/S, Cat. No. 0503). U251 is p53, PTEN mutated glioblastoma cell line with a methylated MGMT promoter, while U87 is p53 wild-type, and PTEN methylated glioblastoma cell line with a methylated MGMT promoter.

2.2 Immunofluorescence

Immunofluorescence analysis was done as described before[117]. Cells were seeded and allowed to grow to 70-80% confluence on coverslips. Cells were briefly washed with 1x PBS twice and fixed with 4% formaldehyde for 10 minutes at room temperature. After that, cells were washed with PBS then blocked for 1 hour with 2% BSA in 1x PBS-Triton X-100 (0.3%). Cells were then incubated with 1:100 Phospho-Histone H2A.X (Ser139) (20E3) (Rabbit mAb #9718 from Cell Signaling), diluted in blocking buffer for one hour. This was followed by incubation with AlexaFluor ® 555 mouse anti-rabbit antibody for another hour for visualization. At the completion of secondary antibody incubation, cells were mounted on the slides with mounting media (Mowiol® mounting media) taken from the microscopy unit at the Cross Cancer Institute, University of Alberta, mixed with 0.1% 4', 6-diamidino-2-phenylindole (DAPI) (Catalog no. D1360, Invitrogen). All the staining procedures were done at room temperature. Washes were carried out

3 times, 5 minutes each with PBS after fixation, primary antibody incubation and secondary antibody incubation. Imaging was performed at 40X magnification (oil immersion) using Carl Zeiss Laser Scanning Microscope. The processing of the images was done using LSM image browser software.

2.3 Semiquantitative PCR

Total RNA was isolated using RNeasy® Mini Kit (QIAGEN) following the protocol from the manufacturer. After that, 1 µg of RNA was used for generating cDNA using reverse transcriptase enzyme and Oligo(dT)12-18 Primer (Invitrogen). After that, the cDNA was amplified using master mix containing Taq polymerase, buffer, nucleotides and primers. Following that, the cDNA was electrophoresed through an agarose gel and stained with ethidium bromide, then visualized. Densitometric analysis of the gels was done using Image J software.

2.4 Primers for Semiquantitative PCR

KAT2A: (GCN5)

Forward Primer: TCTGGGAGTCAGGCTTCAC

Reverse Primer: CAGGTTCTCTGGGAGCGTC

KAT7: (HBO1)

Forward Primer: AGGGCTATGGCAAGATGCTT

Reverse Primer: GCTGACAATGTCCACAGGAT

KAT5: (TIP60)

Forward primer: ACGGCAAGCTGCTGATCGA

Reverse Primer: CTAATCTCATTGATGGTGATC

KAT8: (MOF).

Forward primer: ACAGAAGAACTCAGAGAAGTAC

Reverse primer: CATATTTCATGTACTTGAGGCA

CBP:

Forward primer: CCTCCAAATGGACCCCTGTC

Reverse primer: CCCTGTGACACGCCTGTTT

P300:

Forward primer: CAACAAGAAGAAACCCGGGA

Reverse primer: CAGGTGTAGACAAAGCGGTC

2.5 RT- qPCR

RT- qPCR was done as was described before[117]. Total RNA was isolated using RNeasy® Mini Kit (QIAGEN) following the protocol from the manufacturer. 1 μg of total RNA was used for reverse transcription with Oligo(dT)12-18 Primer (Invitrogen) and Superscript III reverse transcriptase (Vilnius, LT-02241, Applied Biosystems). After that, cDNA Real time quantification of KAT2A, CBP, MOF and Tip60 was assessed using power SYBR Green PCR Master Mix (Applied Biosystems). β-actin was used as the endogenous control. Samples were amplified with a precycling hold at 95˚C for 15 seconds, 30 cycles of annealing and extension at 60˚C for 1 minute. Each measurement was performed with LightCycler@96 (ROCHE) and LightCycler@96

Software. Gene expression was determined using the relative standard curve method normalized to β-actin expression. Histograms are reported as fold change of control which was set at 1.

2.6 Primers for RT-qPCR

KAT2A: (GCN5)

Forward Primer: CCTAAGGAGTATATCGCCCG

Reverse Primer: TCCTTCAGGTGGTTCATCAG

KAT5: (TIP60)

Forward primer: ACGGCAAGCTGCTGATCGA

Reverse Primer: CTAATCTCATTGATGGTGATC

KAT8: (MOF).

Forward primer: CGGTGGAGATCGGAGAAAC

Reverse primer: CTGTACAGCATCCTTCACTG

CBP:

Forward primer: TGGCACGAACATGTCACTCA

Reverse primer: CCATGCGGCGATCCTTTAGA

2.7 Histone extraction

Cells were harvested and labeled according to the treatment done. Cells were then pelleted and washed with 1XPBS then pelleted and resuspended in nuclei isolation buffer and left for 5 -10 min

on ice. Nuclei were pelleted at 5000rpm for 10 min then washed with PBS. Histones were extracted by adding 300 uL of 0.2 M of H2SO4 and vortexing for 30min. The mix was spun at 12500 rpm to precipitate nuclear debris and the supernatant (containing histones) was kept. 1.2 ml of ice chilled acetone was added to the supernatant and incubated at -20ºC overnight then histones were pelleted at 14000 rpm for 20 min. Histones were then washed twice with acidified acetone (prepared by adding 50 mM of HCl to the acetone solution) and then washed with acetone then resuspended in distilled water. Nuclear isolation buffer was prepared as follows: 50 mM Tris - HCl pH 7.5, 250 mM of sucrose, 25 mM of KCl, 5 mM of $MgCl_2$, 0.2 of PMSF, 50 mM of $NaHSO_3$, 45 mM of Na butyrate, 10 mM BME, 0.2% Triton X- 100,. 2 mM of EDTA , 1 mM of sodium orthovanadate and protease inhibitor were added to the buffer.

2.8 Western blots

Western blots were done as described previously[117]. Protein in the samples was quantified by PierceTM BCA (Bicinchoninic acid) protein assay kit (Catalog no. 23227, Thermo Scientific). The samples consisting of whole cell lysate were prepared by boiling 40 µg of protein in 1X loading buffer for 5 minutes. The samples were run on a 7.5% SDS-PAGE and then the proteins were transferred to a polyvinylidene fluoride (PVDF) membrane (Catalog no. 1620177, Bio-Rad) for 70 minutes at 110 V at 4ºC. The membrane was blocked for 1 hour using 5% non-fat dry milk powder in 1x TBST (Tris buffered saline containing 0.1% Tween-20, pH 7.4), and then incubated overnight in primary antibody at 4ºC. Following that, the membranes were washed for 10 min 3 times in TBST and then incubated in 5% non-fat dry milk containing the corresponding secondary antibody linked to Horseradish peroxidase (HRP) for 1 hour at room temperature. The membranes were then again washed 3 times for 10 minutes in TBST and visualized using Western Lighting

Plus ECL (Catalog no. NEL104001, Perkin Elmer) or SuperSignal West Femto (Catalog no. 34095, Thermo Fisher).

Primary antibodies used were bought from Millipore and abcam.

2.9 Assessment the effect of glucose on histone acetylation and the upregulation of histone acetylation after radiation

Cells were cultured in a six well plate for 24-48 hours until they reach 70-80% confluency, then the culture media was changed for another media with different glucose concentrations. After that, the cells were divided into two halves: a half of the cells were harvested directly, while the other half, was irradiated with X-Ray, then harvested. H3 and H4 acetylation was assessed by western blot.

2.10 Testing the effect of glucose deprivation, on DNA repair

U87 cells were cultured in DMEM medium supplemented with 10% FBS, 5% CO_2 and 1% Penicillin/Streptomycin antibiotics in a 24 well plate for 24 hours until they reached 70-80% confluency, then the culture media was changed to culture medium with different amounts of glucose in different wells (as specified), 10% dialyzed FBS and 1% Penicillin/Streptomycin. After that, the cells were irradiated with a 2-gray dose of X-Ray and were left in the same glucose concentrations for either 24 or 6 hours for DNA repair to occur. Immunofluorescence imaging was performed for phosphorylated γH2AX.

2.11 Sulforaphane

R,S-Sulforaphane, dissolved in water, was obtained from LKT Laboratories, Inc. Aliquots of sulforaphane were prepared at a concentration of 50 mg/ml, then diluted in DMEM media into different concentrations (0, 5, 10, 20, 30, 40, 50, 60, 75, 90, 100, 200 uM).

2.12 Sulforaphane treatment

Cells were seeded in 96-well plates at a density of 10,000 cells/well, then left to grow for 24 hours. After that, the media in the wells was replaced with the media containing different concentrations of sulforaphane (0, 5, 10, 20, 30, 40, 50, 60, 75, 90, 100, 200 uM). Cells were incubated with sulforaphane for 24 hours, at 37 °C and 95% O2 / 5% CO2. Cells were then assessed for viability with alamarBlue viability assay.

2.13 alamarBlue cytotoxicity

The relative cytotoxicity of different concentrations of Sulforaphane was established using an alamarBlue assay. Cellular metabolism can be spectrophotometrically measured by examining the difference between the oxidized and reduced state of the REDOX indicator resazurin. Resazurin (oxidized) is blue and non-fluorescent, whereas resorufin (reduced) is red/pink and highly fluorescent. Therefore, by measuring changes in the fluorescence of the dye in intracellular environment, the number of metabolically active cells can be detected. alamarBlue solution (10% [v/v] solution of AB dye) was added into 100 µl of complete media to each well. Cells were incubated with alamarBlue for 1-4 hours, and then fluorescence was measured at the respective excitation and emission wavelength of 540 and 595 nm respectively, using a LUMIstar Omega microplate reader. Viability percentage was normalized to controls (0 uM).

2.14 Invasion Assay

Invasion assay was done as described before[118]. Cell invasion assay was carried out using Transwell® units (8 μm) coated with BD Matrigel Basement Matrix (Corning, Bedford, MA). Cells were added at 5×10^4 per invasion chamber and allowed to invade for 24 h at 37 °C and 95% O_2 / 5% CO_2 towards the lower compartment containing media supplemented with 10% FBS. At completion of the incubation period, non-migrated cells on the upper side of the membrane were removed using a cotton swab. Invading cells were fixed with ice-cold 100% methanol (−20 °C), stained with 0.5% crystal violet and the number of invaded cells analyzed using 10X High Content Microscope and MetaExpress software.

2.15 Cell Cycle analysis with propidium iodide

Culture medium was removed and retained for inclusion of loosely adherent cells. Cells were washed with PBS and then PBS was kept as well. Cells were trypsinized and harvested with the previously saved media. Cells were pipetted up and down to generate a single cell suspension then pelleted at 500 X g for 5 min, and the supernatant was discarded. Following that, the cells were washed with 1X PBS by resuspending the cell pellet in 1 mL 1X PBS, then spinned again at 500 x g for 5 minutes. After that, the cells were fixed with 66% ethanol on ice, by resuspending the cell pellet in 400 μL ice cold 1X PBS, then adding 800 uL ice cold 100% ethanol and mixing well. The cells were then stored at +4ºC for at least 2 hours. After that the cells were taken out and resuspended and pelleted, washed with PBS, then pelleted. Then the cells were stained with Propidium Iodide by gently resuspending the cell pellet in 200 μL 1X Propidium Iodide + RNase Staining Solution, incubating the cells at 37ºC in the dark for 20 – 30 minutes, followed by flow cytometry analysis. Samples were run on the flow cytometer with the appropriate FSC vs. SSC gates to exclude debris and cell aggregates. Analysis was done using the appropriate software.

2.16 Cell viability at different glucose concentrations

U251 and U87 cells were seeded in 96 well plates for 24 hours with a seeding density of 10,000 cells/well, under normal conditions (DMEM, 25 mM glucose, 10% FBS). Astrocytes were seeded on poly-lysine treated 96 well plates with the same seeding density, with Astrocyte media (Components of this media were described earlier.). After that, the medium was removed and the cells were washed with PBS, then the medium was replaced with medium containing different glucose concentrations: (0, 0.25, 0.5, 1, 2, 2.5, 3, 4, 5mM). The cells were incubated in those concentrations for 24 hours, then assessed for viability using the alamarBlue assay mentioned earlier.

2.17 Cell viability in different concentrations of β-Hydroxy Butyrate

Cells were seeded in the same manner as mentioned earlier. β-Hydroxy Butyrate was dissolved in DMEM, and diluted into different concentrations (0, 1, 2, 5, 10, 20 mM). The medium in each well was replaced with medium containing the mentioned concentrations of β-Hydroxy Butyrate, with three wells for each concentration. Three wells had 5 mM glucose concentration as a control. The cells were incubated under those conditions for 24 hours, then viability was assessed using alamarBlue as described earlier.

2.18 Cell viability in different concentrations of β-Hydroxy Butyrate with 2.5 mM glucose

Cells were seeded as described earlier, and the same concentrations of β-Hydroxy Butyrate were prepared, with three wells for each concentration. In addition, 2.5 mM glucose was added to all the wells.

2.19 Cell viability in different glucose concentrations with 5 mM β-Hydroxy Butyrate

Cells were seeded as described earlier, and the same glucose concentrations were added to the media (0, 0.25, 0.5, 1, 2, 2.5, 3, 4, 5mM), in addition to 5 mM of β-Hydroxy Butyrate. Three wells were used for each concentration, and all the wells had 5 mM β-Hydroxy Butyrate.

2.20 Statistical Analysis

GraphPad Prism 5 computer software was used. Data were from at least 3 experiments with a minimum of triplicates for eacher experiment. Values were expressed as mean±SEM. Statistical analysis was performed using one-way ANOVA with Dunnett's Multiple Comparisons Test. Significance is indicated by *($p<0.05$), **($p<0.01$), ***($p<0.001$), or ****($p<0.0001$).

2.21 Imaging details

For the experiments on the number of DSBs, the confocal microscope was set to the following settings: for the DNA DSB experiments, the objective used was plan- Apochromat 40x/1.3 Oil DIC M27. Two channels were used, DAPI channel for the nucleus and Cy3 channel for the γH2AX foci. Pinhole was set at 40 μm for both channels. Pixel dimensions were X: 303.53 and Y: 303.53. Scan mode was one plane, and there were no image stacks acquired in this experiment.

2.22 Foci quantification using Imaris

Imaris software was set as follows: detection of nuclei as cells and foci as vesicles. Cell source = channel 1 (DAPI); cells were detected based on threshold = 202.038, and split by seed points with diameter = 10 μm and number of Voxels above 6058. Vesicles source = channel 2 (Cy3). Vesicles' estimated diameter was above 0.5 μm and their quality was above 670.

2.23 Table of antibodies

Antibody	**Company**	**Catalogue number**	**Dilution recommended**
Anti- phospho-histone H2A.X (Ser139) (Rabbit mAb)	Cell Signaling	9718	1:100
AlexaFluor ® 555 goatanti-rabbit antibody for immunofluorescence	Invitrogen	**A32732**	**1:500**
Recombinant anti-histone H4 (acetyl K5 + K8 + K12 + K16)	Abcam	ab177790	1: 2000
Anti-histone H4 rabbit antibody	Sigma-Aldrich	04-858	1: 3000
Anti-histone H3 antibody	Sigma-Aldrich	05-928	1: 3000
Anti-Histone H3 (acetyl K9 + K14 + K18 + K23 + K27) rabbit antibody	Abcam	ab47915	1:3000

Goat Anti-Mouse IgG (H + L)-HRP Conjugate	BioRad	1706516	1:10000
Goat Anti-Rabbit IgG (H + L)-HRP Conjugate	BioRad	1706515	1:10000

2.24 Table of inhibitors

Inhibitor	**Company**	**Catalogue number**
WM-8014	CAYMAN CHEMICAL	27402
TH 1834	Axon	2339

2.25 Cell irradiation

Cells were irradiated using a Cabinet X-ray irradiation machine Multirad 160 from Faxitron, serial number 2329A60114.

CHAPTER 3: Results

3.0 Results

3.1 Sensitizing glioblastoma cells to radiation by manipulation of histone acetylation

3.1.1 Glioblastoma chromatin state compared to astrocytes

We first wanted to see whether the glioblastoma cells have a more open chromatin state compared to astrocytes as a base line. We used the nuclear volume as an indicator for the chromatin state. The nuclear volumes for both U87 glioblastoma cells and astrocytes were measured under the confocal microscope using DAPI staining. Preliminary data showed that the volume of U87 cells nuclei was much bigger on average than the astrocytes nuclear volume (Figure 3).

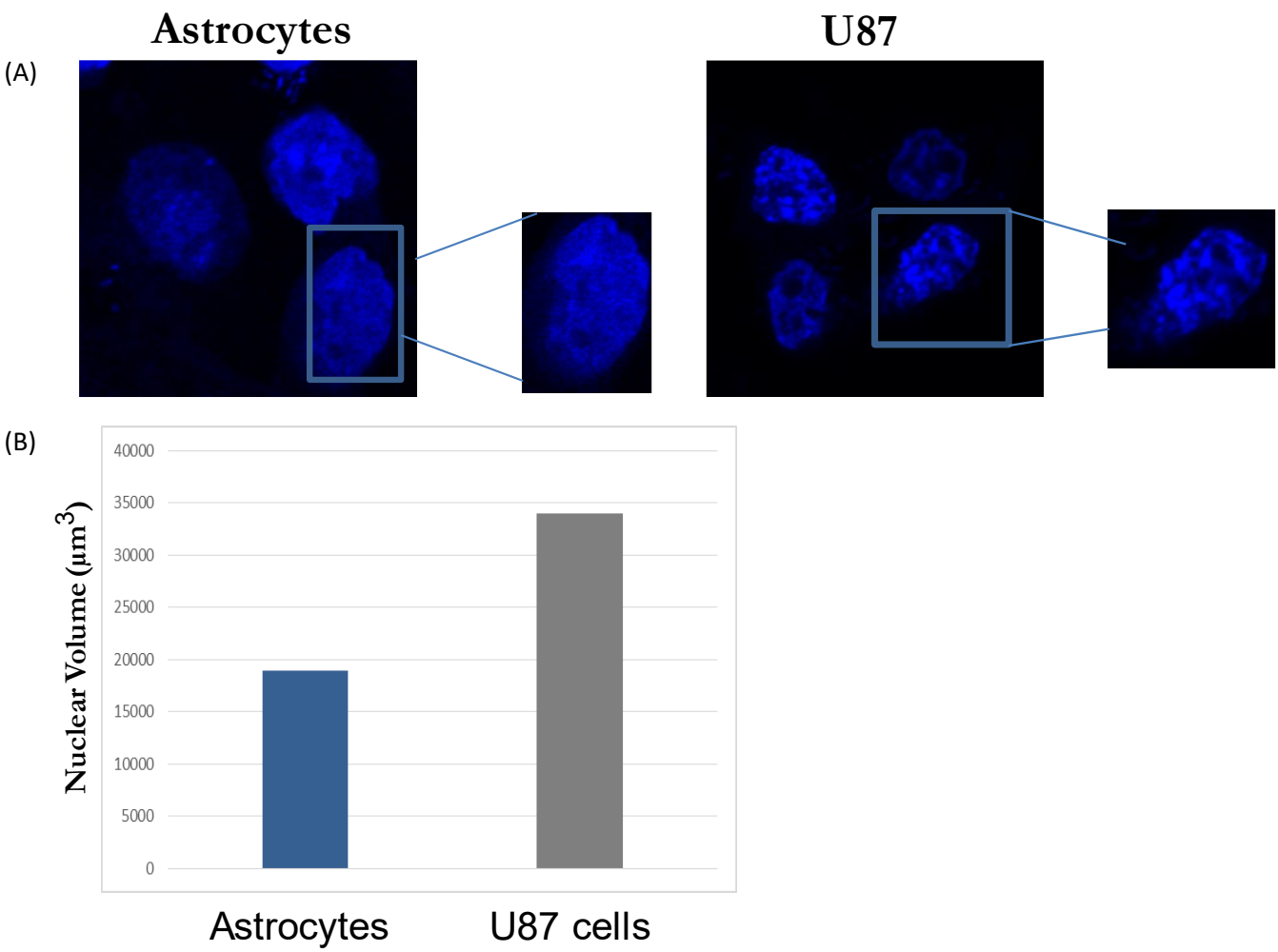

Figure 3: Nuclear volume of glioblastoma cells vs normal astrocytes using DNA staining with DAPI and confocal microscopy. (A) Images of the nuclei of both U87 cells and astrocytes were collected under a 60X objective lens. The nuclear volume of the U87 glioblastoma cells appears bigger compared to that in the normal astrocytes. (B) Quantification of the nuclear volume in U87 cells and normal astrocytes. The nuclear volume in the U87 cells is 2-fold higher compared to normal astrocytes. Bar, 10 µm . n=1.

3.1.2 Semi quantitative and quantitative PCR for HAT genes

We then wanted to compare the baseline expression of different HAT genes in glioblastoma cell lines to astrocytes. The rationale for this was to find if there are certain HAT genes that are upregulated in glioblastoma cell lines compared to astrocytes and use these HAT genes to specifically target the glioblastoma cells. We first performed semi-quantitative PCR on six HAT genes that were found to be upregulated in glioblastoma through Oncomine. Preliminary data showed that GCN5 (KAT2A), HBO1 (KAT7), MOF (KAT8) and Tip60 (KAT5) had a trend for higher expression in GBM lines compared to normal astrocytes. However, we did not see any increase in the expression of CBP (KAT3A) and p300 in the GBM cell lines compared to astrocytes (Figure 4A). After that, RT-qPCR was performed on three of the HAT genes that were upregulated based on semi-quantitative PCR (KAT2A, MOF and Tip60), as well as CBP in both U87 and U251 cell lines, and astrocytes. Preliminary data demonstrated that only KAT5 (TIP60) was consistently upregulated in both U87 and U251 compared to astrocytes (Figure 4B).

(A)

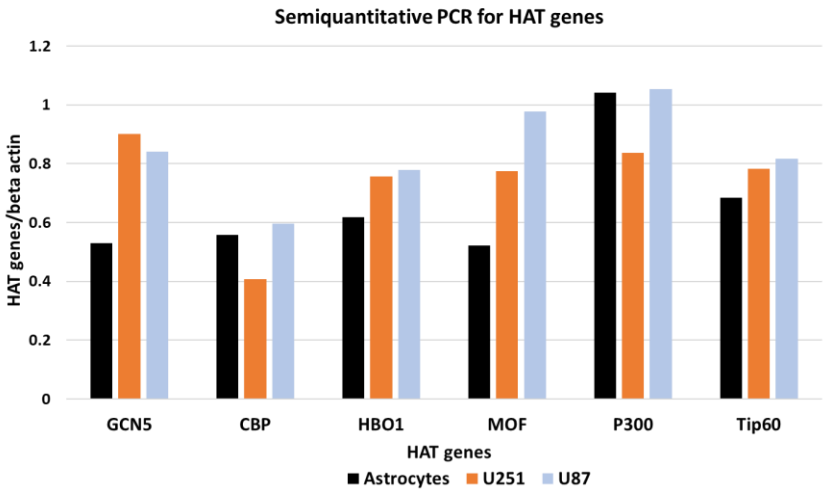

(B)

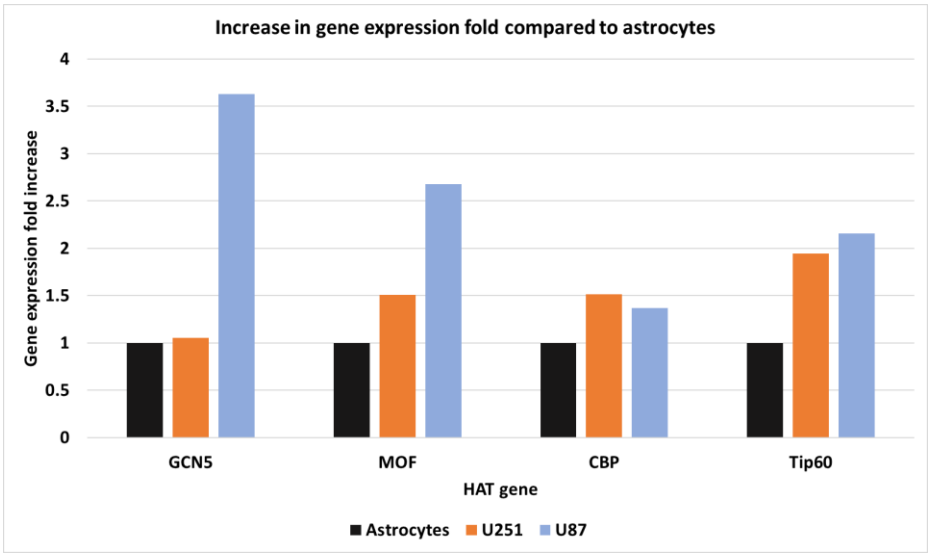

Figure 4: Semiquantitative PCR for HAT genes predicted by Oncomine to be upregulated in glioblastoma. (A): GCN5 (KAT2A), HBO1, MOF and Tip60 showed a trend for higher expression in GBM lines compared to normal astrocytes. We did not see any difference in the expression of CBP and p300 between the glioblastoma cell lines and astrocytes. (B): RT-qPCR was performed on four genes out of the earlier mentioned six genes: GCN5 (KAT2A), CBP, MOF and Tip60. Only Tip60 (KAT5) was consistently upregulated in both U87 and U251 cell lines compared to astrocytes. n = 1.

3.1.3 HAT inhibition's effect on the nuclear volume

We next tested whether a HAT inhibitor can influence the nuclear volume of both U87 cells and astrocytes, and whether we can see a differential effect in their respective volumes. We used the MOF inhibitor from Dr. Michael Hendzel's lab for that purpose. In preliminary experiments, we found that MOF inhibitor could change the nuclear volume in a dose responsive manner in both U87 and astrocytes cell lines. In contrast to our hypothesis, the change in nuclear volume with the MOF inhibitor was very similar in both the U87 cells and the astrocytes. Therefore, we cannot use this for creating a therapeutic window for radiation, using the HAT inhibitor MOF.

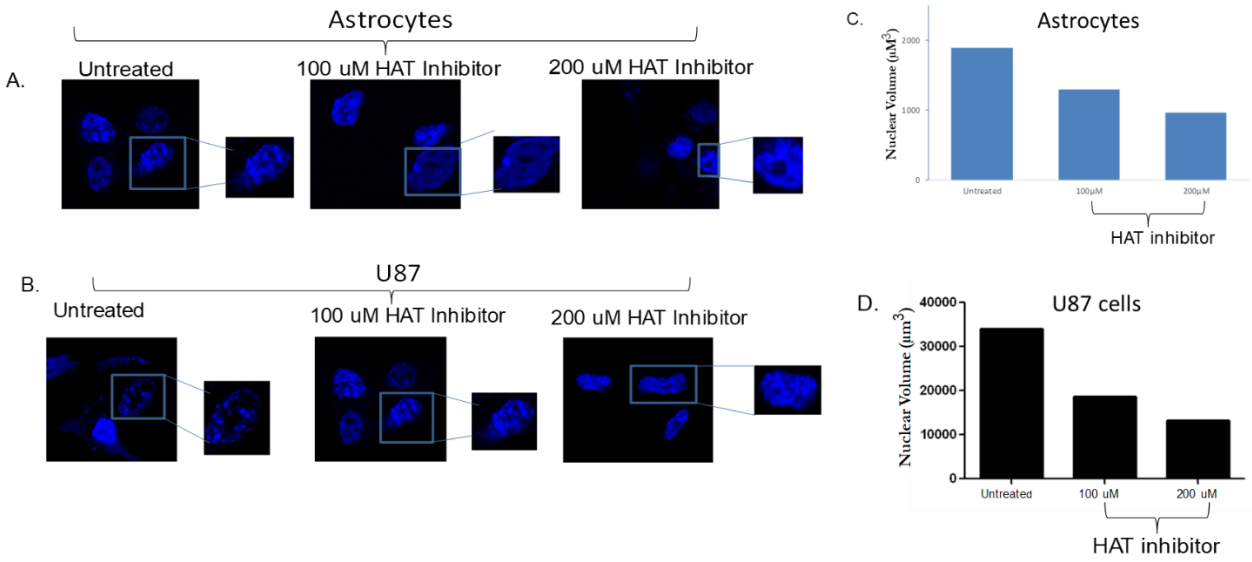

Figure 5: Nuclear volume changes in astrocytes and U87 glioblastoma cells upon treatment with the histone acetyltransferase inhibitor MOF (KAT8). Nuclear volumes of astrocytes (A) and U87 glioblastoma cells (B) decrease progressively upon treatment with the MOF (KAT 8) inhibitor (100 µM and 200 µM). Quantification of the nuclear volumes in the astrocytes (C) and U87 cells (D) with MOF (KAT 8) inhibitor (100 µM and 200 µM) treatment. Bar, 10 mm. n=1.

3.1.4 HAT inhibition effect on the number of γH2AX foci after radiation.

As we did not see any significant changes in HAT gene expression and nuclear volumes between glioblastoma cells and astrocytes, we changed our strategy to sensitizing the glioblastoma cells by affecting DNA repair rather. However, we also kept in mind that the chromatin configuration might influence the effect of the HAT inhibitors on radiation. Therefore, our next experiments used γH2AX for checking the number of double strand breaks foci, which is an indicator of DNA repair efficiency. We used two different HAT inhibitors: WM-8014, and TH1834. WM-8014 is a highly potent inhibitor of histone acetyltransferase KAT6A (MOZ)[119], whereas TH1834 is an inhibitor of KAT5 (Tip60)[120]. WM-8014 was shown to have strong effects in arresting glioblastoma tumor growth[119]. We also included Tip60 inhibitor for two reasons: (1) the Tip60 gene showed an upregulation in our RT-qPCR assay, and (2) Tip60 was shown through multiple studies to have a direct effect on DNA repair (see Introduction). We assessed the number of γH2AX foci in both U87 and U251 cells at two time points: 20 min and 2 hours. The rationale behind the 20 min time point was to assess if the inhibitor influenced the number of DNA double strand breaks (indicated by the number of γH2AX foci) before DNA repair is significant. That is to find out if those inhibitors alter the chromatin configuration and thus change the number of breaks while the DNA repair is still minimal in the first 20 min. On the other hand, the 2 hours time point was done to observe the effect of the inhibitors on the efficiency of the DNA repair. As 70% of the DNA double strand breaks are repaired in the first hour, assessing the number of γH2AX after two hours would tell us if the inhibitor altered the DNA repair efficiency. In one experiment, Tip 60 inhibitor (TH1834) was added to the cells in culture media for 24 hours at the following concentrations: 0, 20, 50, 100 and 200 uM. Following the 24 hours, the cells were subjected to radiation at 2 gray and left for either 20 min or 2 hours, then fixed. 200 uM of TH1834

killed all U87 cells (no images available) and showed large γH2AX foci for U251 cells (Figure 6A). Unexpectedly, preliminary results showed that there was no correlation between TH1834 concentration and the number of γH2AX foci, at both the mentioned time points (Figure 6B). Similar to the Tip60 inhibitor, preliminary data using the MOZ inhibitor (WM-8014) concentration did not show a correlation with the number of γH2AX in both U87 and U251 cells at both the 20 min and the 2 hours time points after radiation (Figure 6D).

A.

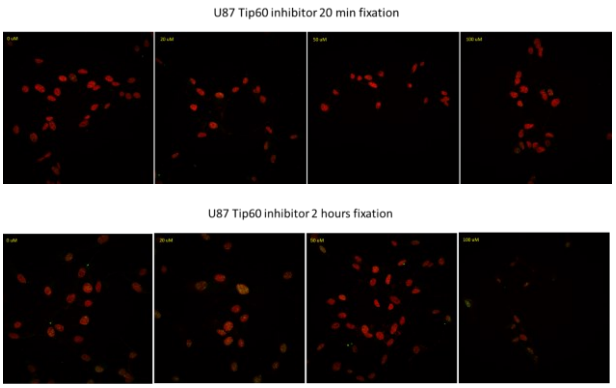

B.

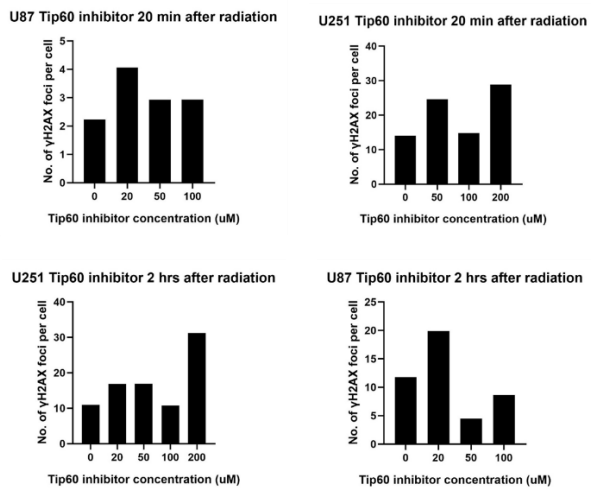

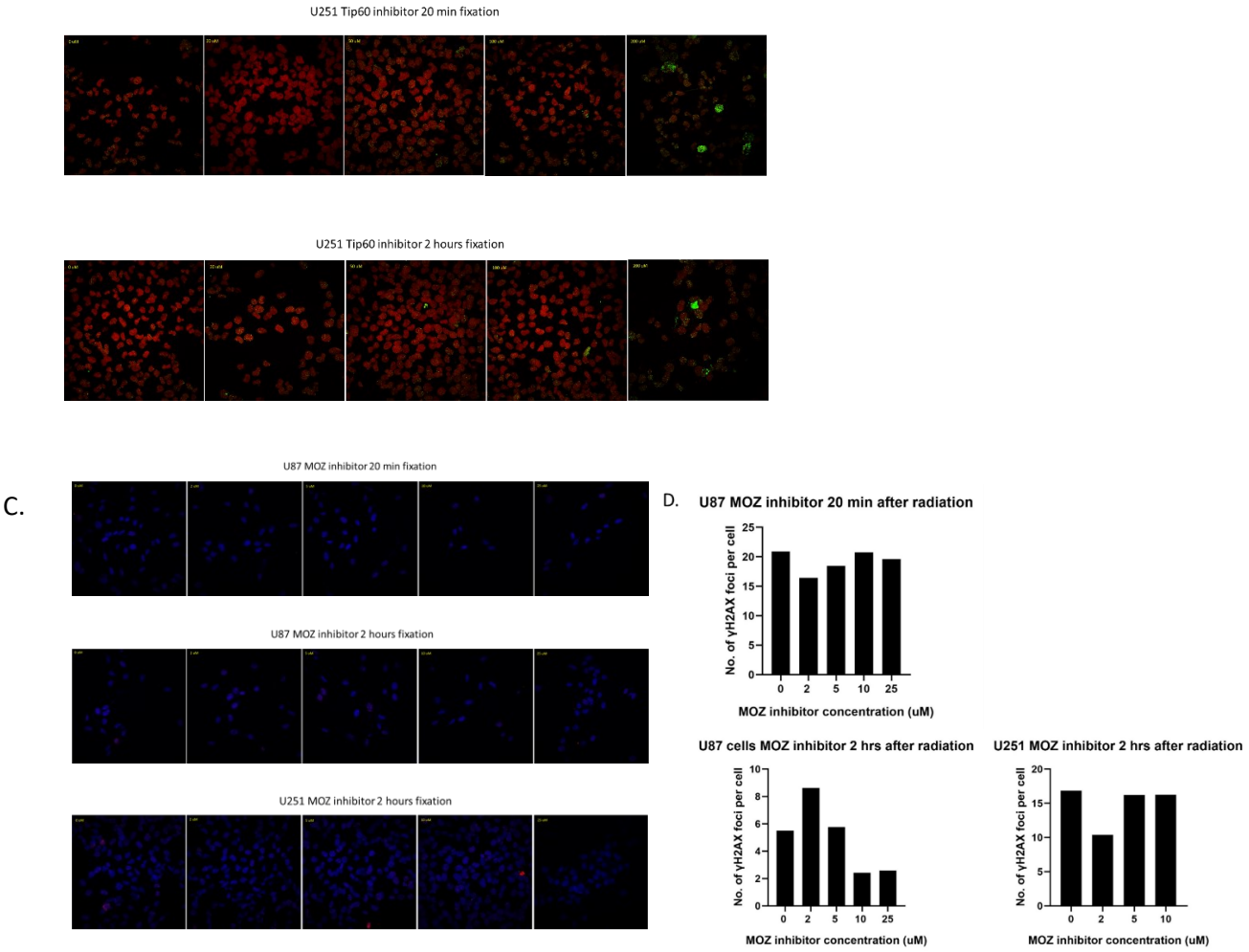

Figure 6. (A): Effect of Tip60 inhibitor and MOZ inhibitor on the number of γH2AX foci after radiation. Immunofluorescence images of both U87 and U251 cells labeled with DAPI and γH2AX antibodies with different TH1834 concentrations. (B): γH2AX foci counted using Imaris software shows no correlation with TH1834 concentrations. (C): Immunofluorescence images of both U87 and U251 cells labeled with DAPI and γH2AX antibodies with different WM-8014 concentrations. (D): γH2AX foci counted using Imaris software shows no correlation with WM-8014 concentrations. All experiments were done one time only (n=1).

3.1.5 The effect of glucose concentration in the medium on histone acetylation

We then used an alternative strategy to alter the histone acetylation. Rather than using different HAT inhibitors which would affect only certain lysine residues, we wanted to alter the pan histone acetylation, with the goal of effectively changing the chromatin configuration and hence impacting the DNA repair. To do so, we aimed at controlling the substrate for histone acetylation, acetyl CoA. Based on the literature, we found that histone acetylation depends on the acetyl CoA that is produced by glucose metabolism. Therefore, we hypothesized that controlling the glucose concentrations in the medium will impact histone acetylation and consequently, DNA repair. We therefore conducted two experiments: (1) We subjected the cells to radiation with a dose of 2 gray, under different glucose concentrations ranging from 0 to 25 mM and assessed the DNA repair efficiency, by counting the number of γH2AX foci. (2) We assessed the level of histone acetylation under either 1 mM or 25 mM glucose (the concentration of glucose in DMEM high glucose media), with or without radiation. First, we assessed pan H3 acetylation in the cells cultured in 25 mM glucose medium vs 1 mM glucose medium. Densitometric analysis of the bands showed that the cells cultured in 25 mM glucose medium had a slightly more acetylated H3 than the ones cultured in no glucose medium (Figure 7B). We followed up with another experiment that included four groups: (1) Cells cultured in 1 mM glucose medium for 24 hours indicated by "NG". (2) Cells cultured in 25 mM glucose medium for 24 hours indicated by "FG". (3) Cells cultured in 1 mM glucose medium for 24 hours then radiated with 2 gray indicated by "NGR". (4) Cells cultured in 25 mM glucose medium for 24 hours then radiated with 2 gray indicated by "FGR". All cells (both irradiated and non-irradiated) were left for an hour then harvested for western blots. The literature shows that radiation stimulates histone acetylation and that glucose starvation inhibits radiation-induced histone acetylation[90]. Therefore, we wanted to test if glucose starvation would impair the

radiation induced histone acetylation in glioblastoma cells, and hence affect the DNA repair. As shown in Figure 7C, both U87 and U251 cells were tested for H3 acetylation, and U251 cells were tested for H4 acetylation. We did not observe any significant changes in the level of acetylation with the changes in glucose concentration in either irradiated or non-irradiated cells. Moreover, we did not notice any induction of acetylation caused by radiation (Figure 7D). To determine the effect of glucose concentration on the DNA repair, cells were cultured in different glucose concentrations for 24 hours to deplete their acetyl CoA levels, then irradiated. After that, the cells were left to recover for either 6 or 24 hours under the same glucose concentrations then fixed and stained for immunofluorescence with γH2AX antibodies. We did not observe significant differences in the number of γH2AX foci among cells treated with different glucose concentrations after both fixation points (6 hours and 24 hours) (Figure 7).

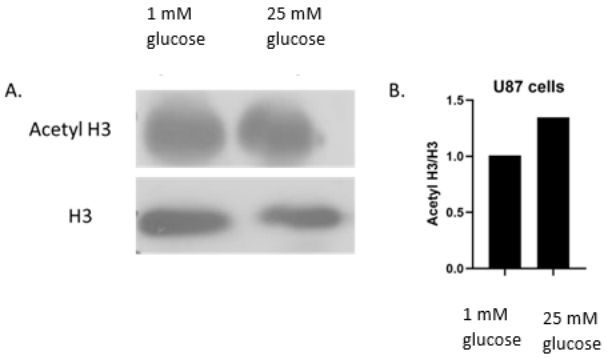

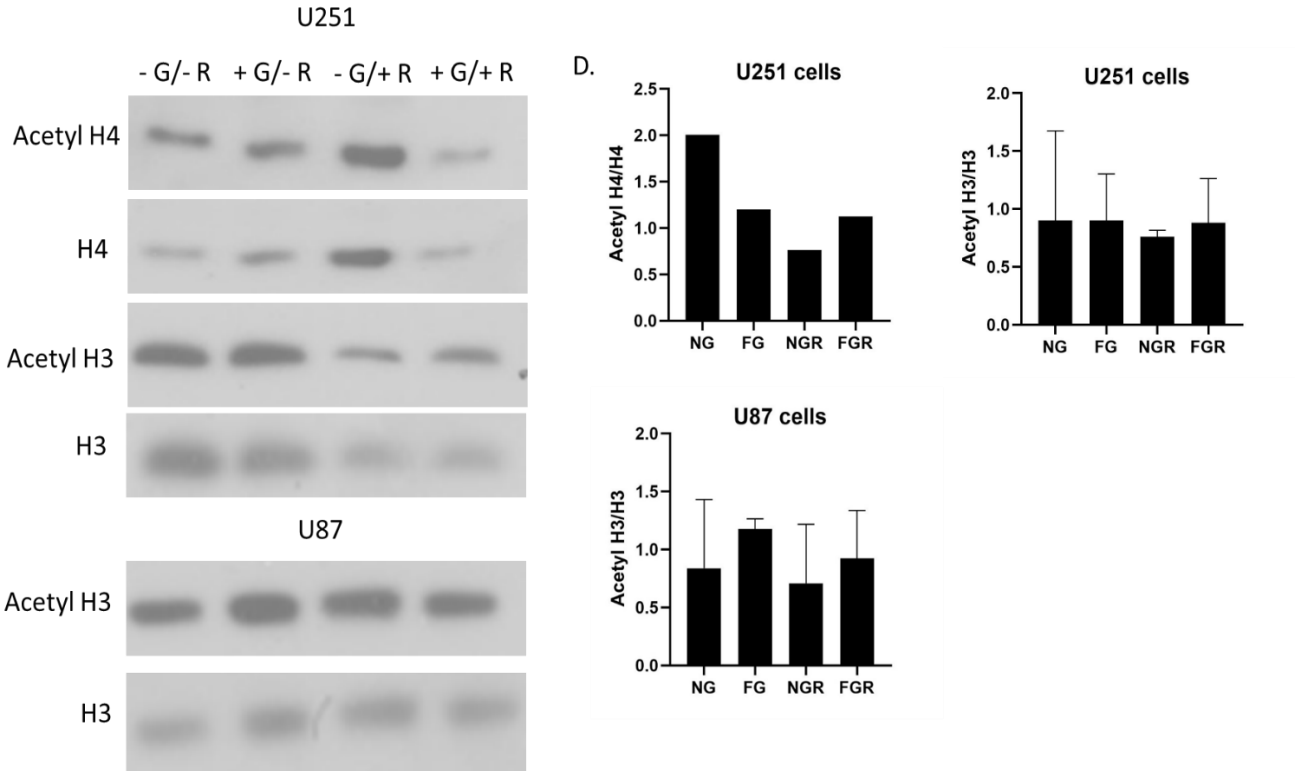

Figure 7. The effect of glucose concentration changes in the media on histone acetylation. (A): Western blot data with antibodies against Acetyl H3 and H3, from cells cultured either in 25 mM glucose or a 1 mM glucose. (B): Dosimetry analysis of the blot showed in (A) shows slightly higher acetylation in the cells cultured in rich glucose vs the cells cultured in 1 mM glucose. (C): Western blot data with antibodies against Acetyl H3, H3, acetyl H4 and H4 from U251 and U87 cells. -G, +G, -R and +R indicate no glucose, 25 mM glucose, no radiation and radiation with 2 gray, respectively. (D): Dosimetry analysis of the blot shown in (C) shows no significant difference in acetylation between the conditions shown in the blot. NG, FG, NGR and FGR denotes 1 mM glucose, full glucose (25 mM), 1 mM glucose + radiation (2 gray), and full glucose + radiation, respectively. n = 3 for H3 and n =1 for H4 experiments.

A.

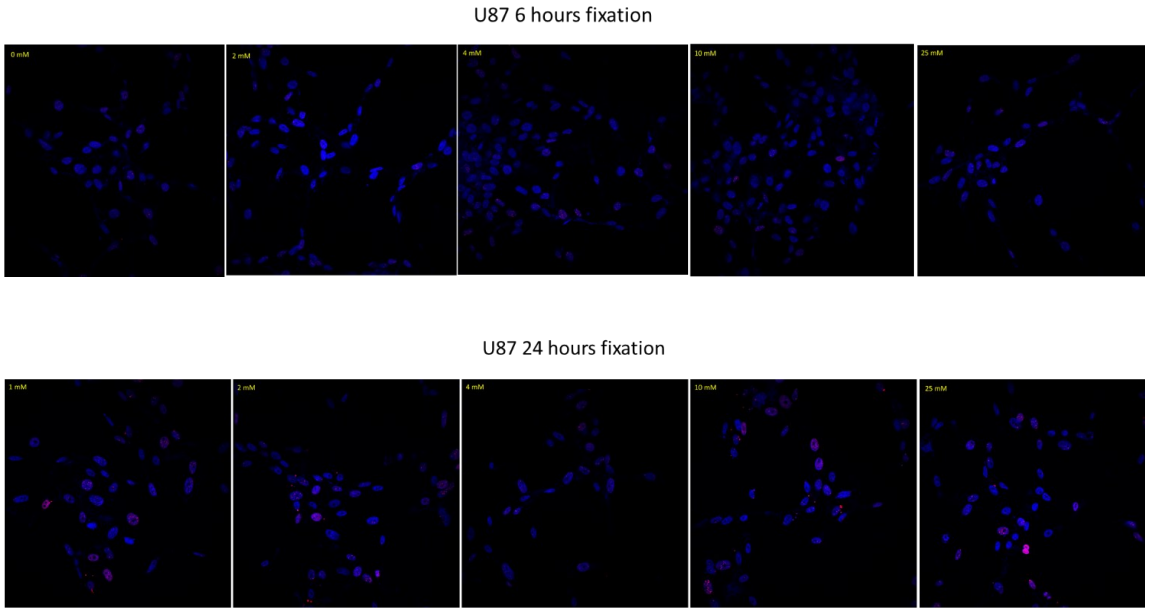

B.

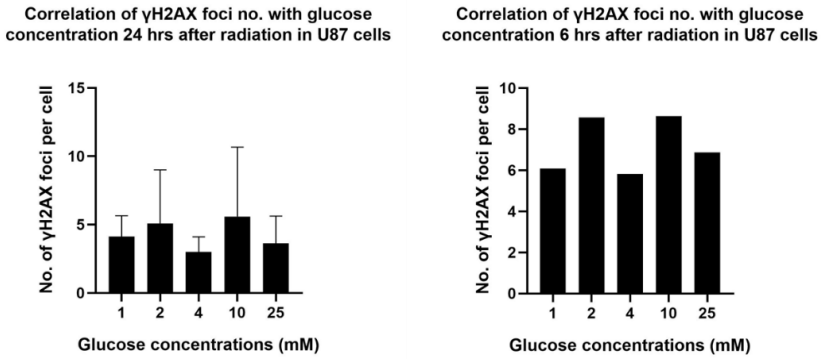

Figure 8: The effect of glucose concentrations on the number of γH2AX after radiation. (A) Immunofluorescence images of U87 cells labeled with DAPI and γH2AX antibodies with different glucose concentrations. (B) γH2AX foci counted using Imaris software shows no correlation with glucose concentrations. n= 3 for the 24 hours time point and n= 1 for the 6 hours time point.

We questioned whether there might be an alternative source for acetyl CoA other than glucose. A review of the literature showed that glioblastoma could be an exception from the other cancers that use the glucose as a source for acetyl CoA for histone acetylation, however its source of the acetyl CoA is still unknown.

The other alternative to using glucose-free medium would be to treat cells with a ketogenic media. Ketogenic diet medium is a glucose-free medium that contains 5 mM β-Hydroxy Butyrate. The rationale behind this strategy change is that gliomas have: (1) impaired mitochondrial function, and (2) less active OXCT1 3-oxoacid-CoA transferase 1. Therefore, we thought we could induce tumor cell-selective energy deprivation by using the ketogenic diet, where normal astrocytes could metabolize the β-Hydroxy Butyrate, with glioblastoma cells lacking the capacity to do so. Consequently, this would induce tumor selective energy deprivation, leading to tumor growth arrest.

3.1.6 Glioblastoma cell lines cannot survive without glucose

To assess the effect of ketogenic diet on glioblastoma cells, we firstly assessed the glucose concentration necessary for glioblastoma cells to survive. We observed that U251 cells needed 2 mM of glucose to sustain 100% survival, while they needed only 0.5 mM of glucose for 50% survival. Moreover, U87 needed 2.5 mM glucose for survival of all the cells, and 1 mM for 50% survival. On the other hand, astrocytes only needed 0.25 mM glucose for 100% survival for 24 hours. This comes as no surprise as it is well known that cancer cells have a stronger need for glucose and a faster metabolism (Figure 9).

A.

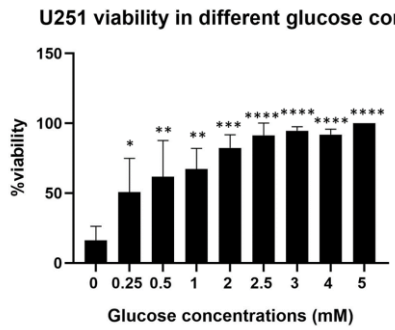

B.

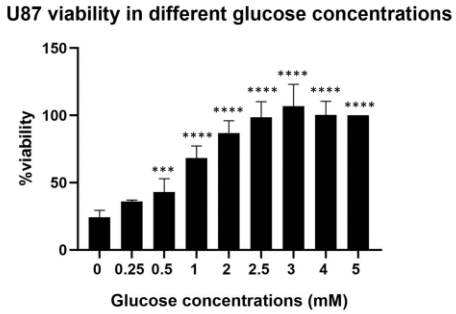

C.

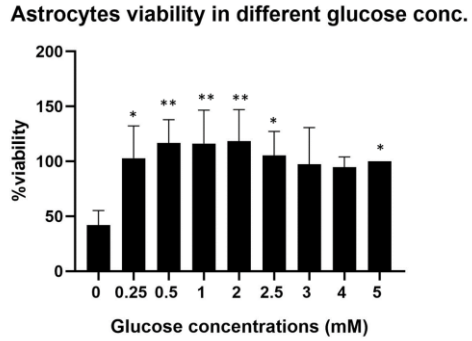

Figure 9. The alamarBlue assay was used to determine the percentage viability of both U251 and U87 cell lines, and astrocytes. The percentage was determined by denoting the average viability of three different cell culture experiments under 5 mM glucose as 100%, then comparing all cell viability to that value. U251 cells showed 100% survival in 2 mM glucose for 24 hours, with 0.5 mM glucose required for 50% survival (A). U87 needed 2.5 mM glucose for survival of all the cells, and 1 mM glucose for 50% survival (B). On the other hand, astrocytes only needed 0.25 mM glucose for the whole population to survive for 24 hours (C). One-way Anova Dunnett's Multiple Comparison test was performed with 0 mM as a control.

3.1.7 Glioblastoma cells did not survive when cultured in different β-Hydroxy Butyrate concentrations and no glucose media.

We next wanted to test whether glioblastoma cells can metabolize β-Hydroxy Butyrate. For both the U251 and U87 cell lines, we found no significant correlation between cell viability and β-Hydroxy Butyrate concentrations. In fact, there was no difference in survival between cells cultured in 0 mM of β-Hydroxy Butyrate and in 20 mM. However, there was a significant difference in survival between cells cultured in medium with 5 mM of glucose and the cells cultured in medium with only β-Hydroxy Butyrate. In comparison, astrocytes showed more viability without glucose (50%), but there was no difference between 0 mM β-Hydroxy Butyrate and 20 mM, indicating that β-Hydroxy Butyrate wasn't advantageous to astrocytes either (Figure 10).

A.

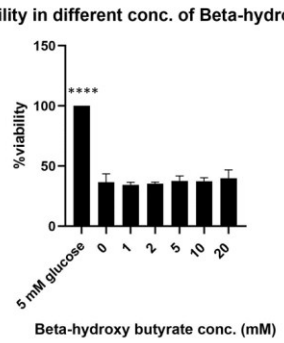

B.

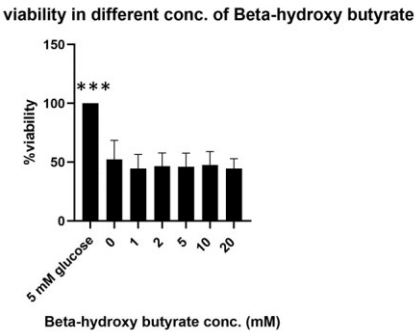

C.

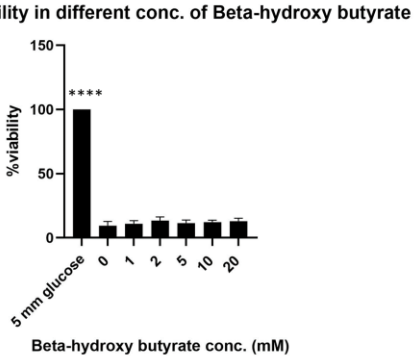

Figure 10. The alamarBlue assay was used to determine the percentage viability of both U251 and U87 cell lines, and astrocytes. For both U251 and U87 cells, there was no significant correlation between cell viability and β-Hydroxy Butyrate concentrations (A, C). There was no difference in survival between cells cultured in 0 mM β-Hydroxy Butyrate versus 20 mM. However, there was a difference in survival between cells cultured in 5 mM glucose and the cells cultured with only β-Hydroxy Butyrate. Astrocytes showed more viability without glucose (50%), but there was no difference in cell viability in cells cultured in 0 mM β-Hydroxy Butyrate and 20 mM, indicating that β-Hydroxy Butyrate wasn't advantageous to astrocytes either. n=3 for all experiments. One-way Anova Dunnett's Multiple Comparison test was performed with 0 mM β-Hydroxy Butyrate as a control.

3.1.8 β-Hydroxy Butyrate showed no difference in survival upon adding 2.5 mM glucose

We hypothesized that if we gave the cells a minimum dose of glucose (2.5 mM), they might be able to use β-Hydroxy Butyrate to boost their growth. However, we did not find any significant effect of β-Hydroxy Butyrate on cell viability. None of the cells (U251, U87, astrocytes) were able to gain any growth advantage using β-Hydroxy Butyrate (Figure 11).

A. U251 viability in different conc. of beta-hydroxy butyrate with 2.5 mm glucose

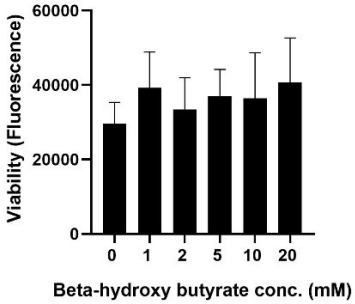

B. U87 viability in different conc. of beta-hydroxy butyrate with 2.5 mm glucose

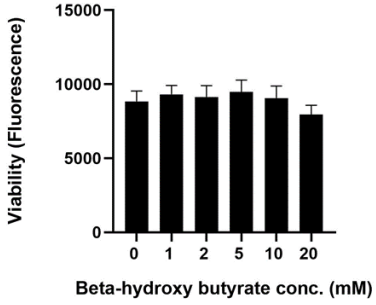

C. Astroc viability in different conc. of beta-hydroxy butyrate with 2.5 mm glucose

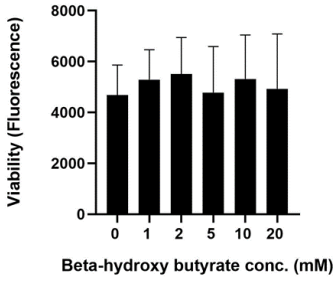

Figure 11. AlamarBlue assay was used to determine the percentage viability of both U251 and U87 cell lines, and astrocytes. No significant effect of β-Hydroxy Butyrate was found on cell viability, upon addition of 2.5 mM glucose. n = 3.

3.1.9 Cell viability curve with different glucose concentrations and 5 mM β-Hydroxy Butyrate.

Finally, we tested if the cells will be able to survive on a lower dose of glucose if it was combined with 5mM β-Hydroxy Butyrate (Figure 12). However, we did not find a significant difference in cell viability in the presence of β-Hydroxy Butyrate, compared to glucose alone as shown in (Figure 12).

A.

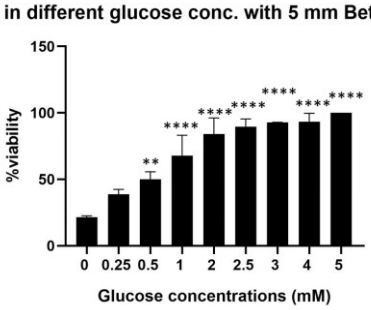

B.

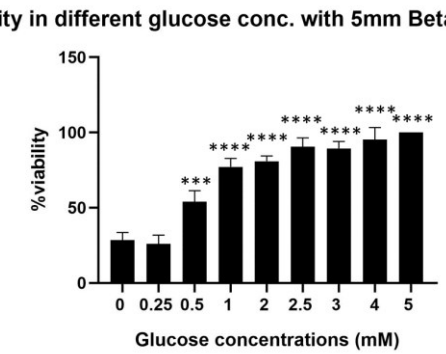

C.

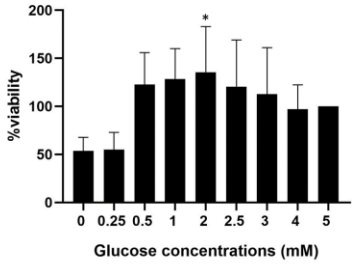

Figure 12. Cells were seeded in different doses of glucose, combined with 5mM β-Hydroxy Butyrate. AlamarBlue assay was used to determine the percentage viability of both U251 and U87 cell lines, and astrocytes. The percentage was determined by considering the average viability of three different cell culture experiments under 5 mM glucose + 5 mM β-Hydroxy Butyrate as 100%, then comparing all the viability results to that value. No significant impact on the cells' viability was found by adding the β-Hydroxy Butyrate, compared to glucose alone. One-way Anova Dunnett's Multiple Comparison test was performed with 0 mM being the reference point. n=3, $P < 0.01$ denoted by **, $P < 0.001$ denoted by ***, $P < 0.0001$ denoted by ****.

3.2 Sulforaphane as an alternative therapy for glioblastoma.

3.2.1 Cytotoxic effect of sulforaphane on glioblastoma cell lines at a relatively low dose

We first observed the morphology of U251 cells cultured with different concentrations of sulforaphane. We seeded the cells in 6 well plate for 24 hours then added the sulforaphane (0, 10, 30, 50, 70 and 90 μM final concentrations) for 24 hours. The cells were photographed under the light microscope. We observed that the cell morphology changed as a function of increased sulforaphane dose from cells with extended and spread borders to a more circular and confined shape (Figure 13A). The cells started to lose their normal morphology starting with 30 μM sulforaphane, with completely lysis observed when cells were cultured in 90 μM sulforaphane (Figure 13A). Following that, we quantified the cells' viability using the alamarBlue assay. We observed that sulforaphane started to have a significant effect on cell viability in both U251 and U87 cell lines at concentrations ≥ 30 μM, consistent with our cell morphology study under the light microscope. Sulforaphane had a cytotoxic effect on U251 and U87 cells with an LD50 of 75 μM and 40 μM for U251 and U87, respectively (Figures 13B and C). The cell viability inversely correlated with the increase in sulforaphane concentration, indicating a dose dependent cytotoxicity for glioblastoma cells to sulforaphane. We next asked whether sulforaphane affected normal cells in the same dose range, which would create a therapeutic window to allow us to investigate it as a viable treatment for glioblastoma. Since glioblastoma is a brain cancer, we chose to test sulforaphane on astrocytes, which are very abundant in the brain and easy to culture and passage for enough time to be tested. In addition, we also tested sulforaphane on fibroblasts, being the most abundant connective tissue cell type found throughout the body[121]. We found that

sulforaphane started to have a significant effect on astrocyte viability at concentrations greater than 100 µM with an LD50 at a very high sulforaphane dose (175 µM), showing that sulforaphane could be a promising agent for brain tumors. However, sulforaphane was toxic for fibroblasts at a lower LD50 (50 µM) (figure 14). Nonetheless, in vivo studies need to be done to accurately assess the toxicity of sulforaphane.

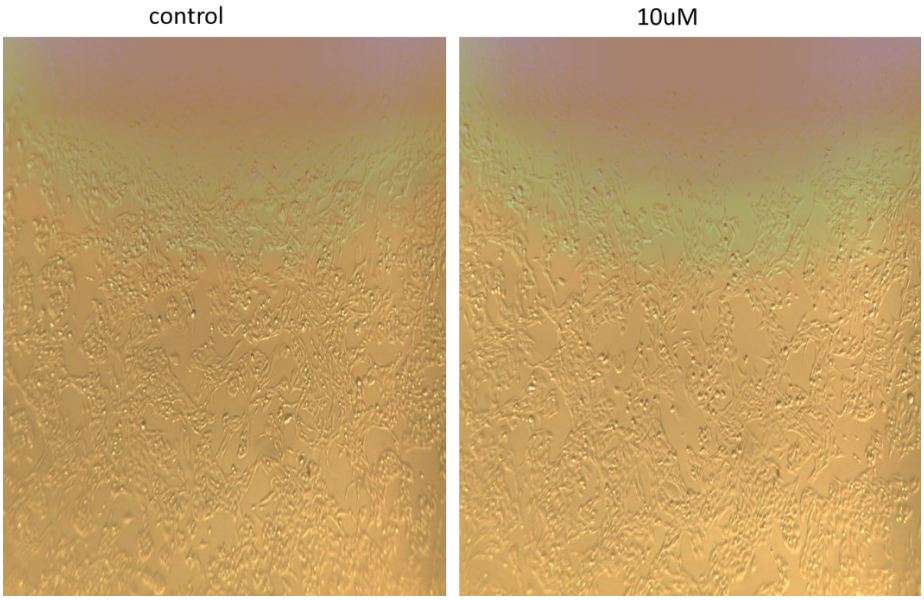

30uM

50uM

30uM

50uM

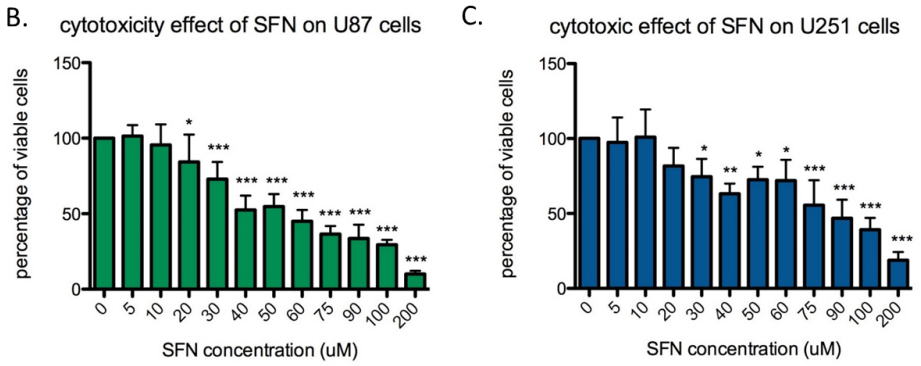

Figure13. Sulforaphane exerted a cytotoxic effect on U87 and U251 cells. (A) Sulforaphane changed the cell morphology and lysed U251 cells in a dose dependent manner as shown under light microscope. Sulforaphane had a cytotoxicity effect with an LD50 of 75 µM and 40 µM for U251(B) and U87(C), respectively. A dose-response effect was observed. Statistics were done using Anova One Way Analysis; Dunnett's Multiple Comparison Test, n =3. $P<0.05$ denoted by *, $P < 0.01$ denoted by **, $P < 0.001$ denoted by ***, $P < 0.0001$ denoted by ****.

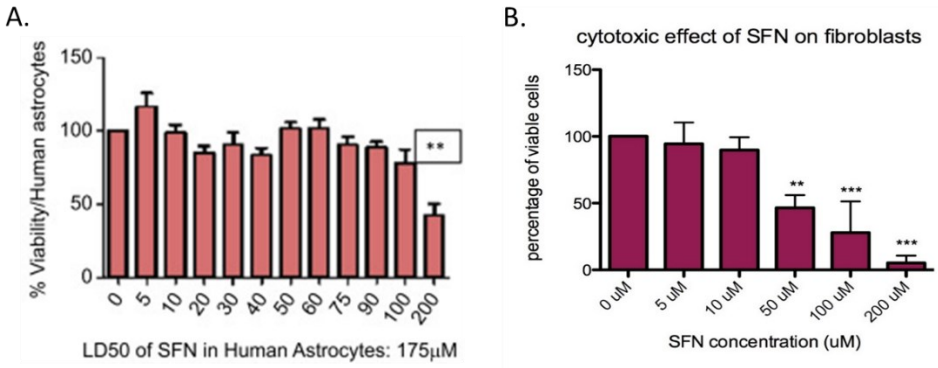

Figure14. Sulforaphane exerted a cytotoxic effect on fibroblasts and astrocytes. Sulforaphane had a cytotoxicity effect on fibroblasts with an LD50 of 50 μM (A) and a cytotoxic effect on astrocytes with an LD50 of 175 μM (B). A dose-response effect was observed. Statistics were done using One Way Analysis; Dunnett's Multiple Comparison Test, n =3. $P<0.05$ denoted by *, $P < 0.01$ denoted by **, $P < 0.001$ denoted by ***, $P < 0.0001$ denoted by ****.

3.2.2 Sulforaphane inhibited U87 invasion in a significantly low dose.

Next, we assessed sulforaphane's anti-invasion effect on U87 cells. U251 cells are not invasive[122], therefore, they were excluded from this experiment. Sulforaphane significantly inhibited U87 invasion at a very low dose (5 μM). In addition, at 40 and 60 μM doses, sulforaphane almost completely inhibited invasion of glioblastoma cells. This shows that sulforaphane can be a beneficial adjuvant therapy for glioblastoma (Figure 15).

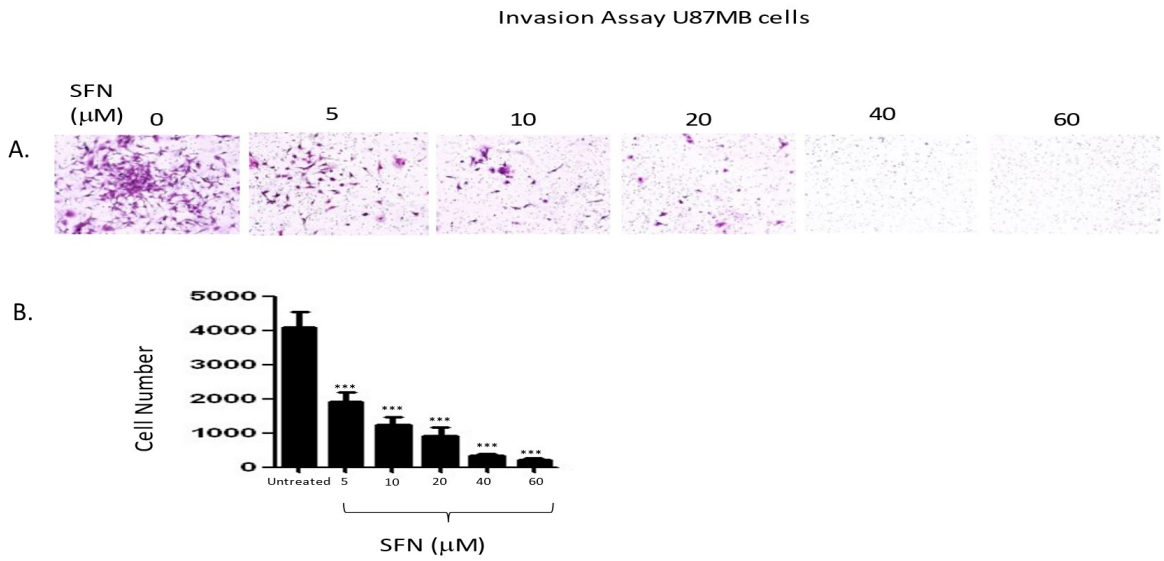

Figure15. Invasion assay shows the effect of sulforaphane on U87 cells invasion. Approximately 50,000 cells were seeded in a 24 well plate with Matrigel inserts. The cells were treated with different concentrations of sulforaphane (μM) for 48 h at 37C/5%CO2 incubation. Invaded cells were fixed with ice-cold 100% methanol (−20 °C), stained with 0.5% crystal violet and invaded cells were counted under 10X magnification using a High Content Microscope (A). The images were analyzed using MetaExpress software, the results showed that sulforaphane significantly inhibited cell invasion ($p<0.001$), in a dose-dependent manner (B). Stats were done using One Way Analysis; Dunnett's Multiple Comparison Test, n =3. $P<0.05$ denoted by *, $P < 0.01$ denoted by **, $P < 0.001$ denoted by ***, $P < 0.0001$ denoted by ****.

3.2.3 Sulforaphane caused U251 cell cycle arrest

Our next experiment sought to determine the effect of sulforaphane on cell cycle. Propidium iodide flow cytometry was used to determine the cell cycle phase of U251 cells after being treated with different concentrations of sulforaphane for 24 hours versus control. Sulforaphane increased the percentage of cells in the G2 phase of cell cycle at 30 μM from 14.7% (Control) to 40%. While preliminary (n=1) these data suggest that sulforaphane causes cell cycle arrest (Figure 16).

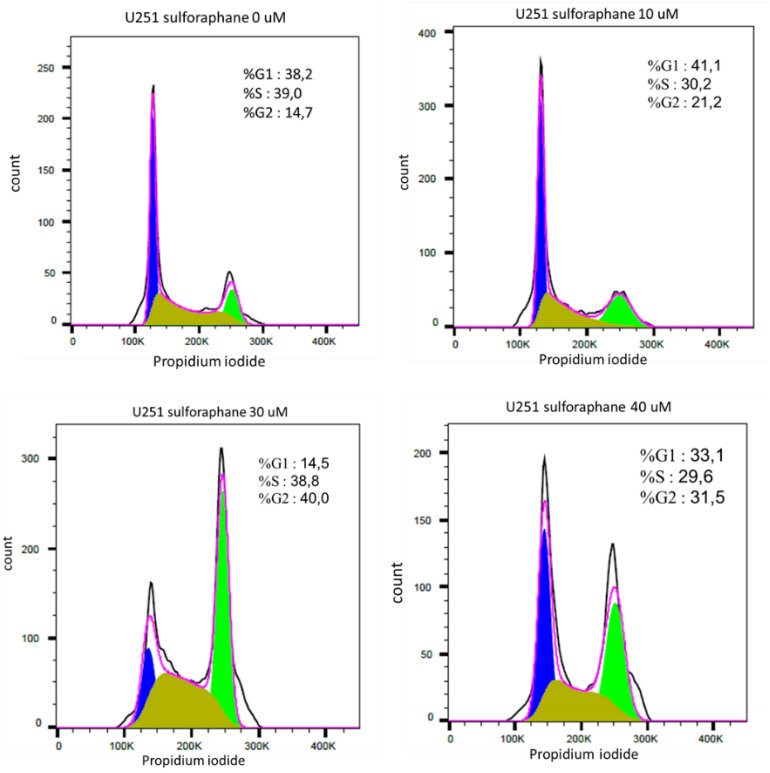

Figure 16. Cells were seeded and left to settle for 24 hours, then the medium was replaced by medium containing 0, 10, 30 and 40 µM of sulforaphane. Cells were stained with propidium iodide and harvested for flow cytometry cell cycle analysis. At 30 a 40 µM of sulforaphane, the percentage of cells in G2 phase increased drastically, indicating cell cycle arrest. n= 1.

Sulforaphane was found to be an HDAC inhibitor in several research papers in other cancers but not in glioblastoma[106,123]. We questioned whether sulforaphane is also an HDAC inhibitor in glioblastoma cells. Therefore, we tested the upregulation of H3K27 acetylation in response to sulforaphane addition, as a measure of sulforaphane's HDAC inhibition. Preliminary data demonstrated that sulforaphane increased the acetylation of H3K27 at a very low concentration (20 µM) (Figure 17).

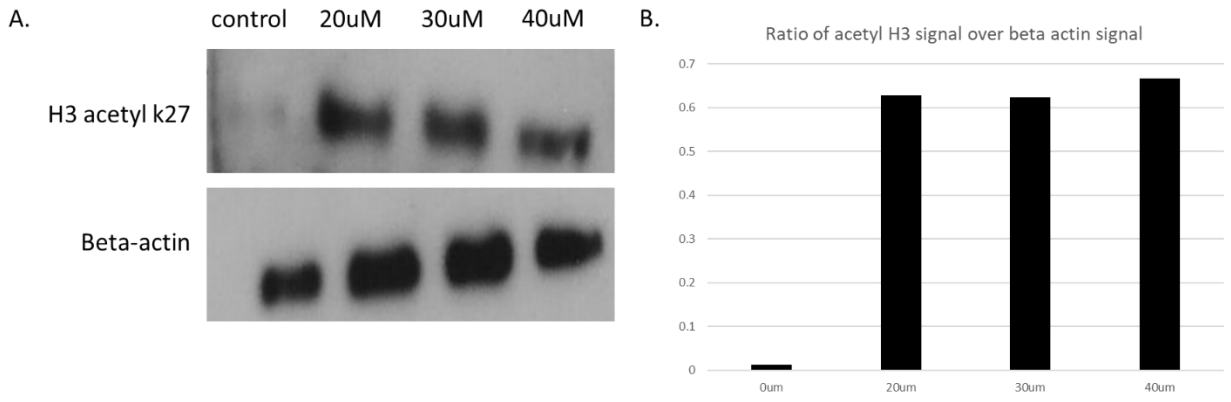

Figure 17. Western blot experiment using antibodies for H3 acetyl K27, and beta-actin as control. (A) Western blot bands show an upregulation of H3K27 acetylation with the addition of sulforaphane. (B) Densitometric analysis was done on the bands using ImageJ software showed an increase in density of the bands upon increasing the dose of sulforaphane. n=1.

Since histone deacetylase inhibitors were shown to increase the sensitivity of cancer cells to radiation[124], we tested the synergy of the combination of sulforaphane with radiation. We used alamarBlue to assess the viability of U87 and U251 cells after being subjected to different combinations of sulforaphane and radiation and left for 24 hours. We found that sulforaphane decreased the viability of cells in a dose dependent manner as has been observed previously. However, there was no significant differences between sulforaphane doses combined with either 0 gray or 2, 6 and 10 gray of radiation. This shows that there was no synergy between sulforaphane and radiation in affecting the cell viability. However, it is well known that metabolic tests, alamarBlue being one of them, are not very efficient in assessing the effect of radiation on the cells. Therefore, our next step is to assess this combination using clonogenic assays, which is an ongoing experiment at the moment.

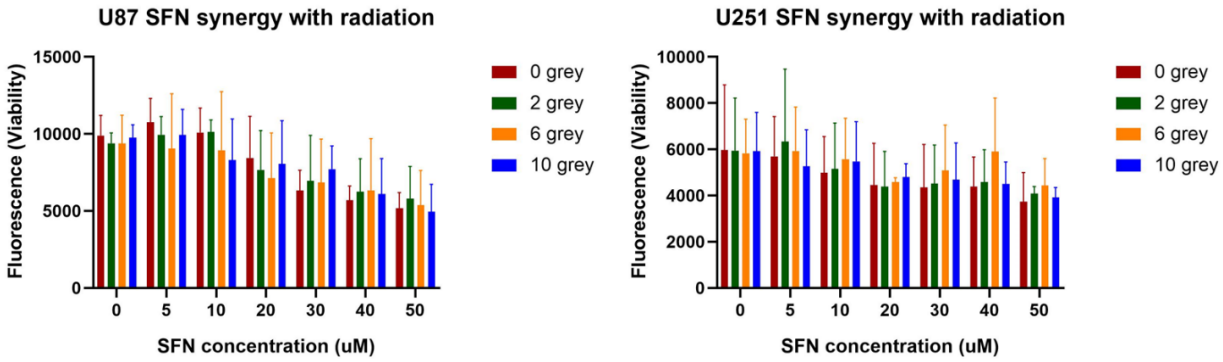

Figure 18. Sulforaphane synergy with radiation experiment using alamarBlue assay. Sulforaphane was tested for synergy with radiation. AlamarBlue was used to assess the viability of U87 and U251 cells after being subjected to different combinations of sulforaphane and radiation and left for 24 hours. Sulforaphane decreased the viability of cells in a dose effective manner. There were no significant differences between sulforaphane doses combined with either 0 gray or 2, 6 and 10 gray of radiation. This shows that there was no synergy between sulforaphane and radiation in affecting the cell viability that can be detected with alamarBlue. Two-way Anova was done to compare the different groups. n=3.

CHAPTER 4: Discussion

4.0 Discussion

Glioblastoma (glioblastoma) is one of the most devastating cancers, with a very bad prognosis and extremely low survival rate[4]. The current interventions including surgery, radiation and temozolomide are merely delaying the inevitable, and barely increases the patient's quality of life[5]. Second line treatments like bevacizumab or tyrosine kinase inhibitors, did not show an improvement in survival rates[58–62]. Glioblastoma was also found to be resistant to immunotherapy, despite its significant success in other cancers[7]. Therefore, the need for new treatments is extremely urgent.

As mentioned above, the main treatment for glioblastoma is radiation therapy. The majority of patients around the world go through radiation therapy for both primary brain tumors and secondary ones that originate from extracranial tumors, which makes radiation an indispensable treatment for the majority of brain tumors[125].

Despite it being essential, radiation therapy has been shown to have permanent and substantial cognitive side effects in a significant percentage of the patients (50 to 90%). The affected cognitive functions involve memory, learning, attention and executive function[125]. The most common neurotoxic symptom of radiation is diffuse cerebral injury[126]. A minority of patients might experience radiation induced necrosis at high doses and increased fraction size, with lower probability at low doses. Radiation induced necrosis also increases significantly with the use of chemotherapy[127].

These findings indicate that it is absolutely crucial to find adjuvant therapies that could protect normal tissue from radiation, or increase the sensitivity of glioblastoma tissue to radiation, which would enable the dose of radiation therapy to be reduced, minimizing its toxic side effects.

In this study, we explored multiple approaches to exert cytotoxic effects on glioblastoma and sensitize the glioblastoma cells to radiation while keeping the normal tissues intact. We sought to target the specific cancer traits, which differentiate the cancer tissue from the normal tissue, such as a requirement for rapid replication, transcription and altered gene expression. Our proposal was based on several evidence-supported hypotheses: (1) We firstly speculated that chromatin condensation would decrease the radiation mediated DNA damage in the condensed areas. This was based on multiple studies reporting that the heterochromatin regions are less susceptible to DNA damage by ionizing gamma radiation than open euchromatin regions[128,129]. The reason for that phenomenon is thought to be the presence of higher amount of DNA- binding proteins in the chromatin condensed areas that act as a shield to gamma radiation by reducing the accessibility of radicals to the DNA, and themselves reacting with these radical[129]. (2) We further hypothesized that the inhibition of HATs would induce a more condensed chromatin form. This was based on a key piece of information that was well established in the literature; the acetylation of lysine residues, on the tails of histones that[96] comprise the nucleosomes of the chromatin catalyzed by histone acetyltransferases (HATs), neutralizes the positive charge on the lysine, and therefore reduces the affinity between DNA and the acetylated histone residues. This process results in loosening the chromatin, enhancing the accessibility of transcription factors to the DNA[18]. (3) HATs are required for replication[130], and therefore, would be in extra need in cancer cells.

Based on these three key research findings, we proposed that inhibition of HATs would induce a closed chromatin structure in both normal cells (astrocytes in this study) and cancer cells (glioblastoma cells), which would protect the cells from radiation- mediated DNA damage. However, because glioblastoma cells are in extra need for HAT enzymes due to their fast-paced replication, they would resist the HAT inhibition, and therefore maintain an open chromatin

configuration, rendering them extra sensitive to radiation. We started out our study by testing the effect of HAT inhibitors on the chromatin structure. However, in an initial experiment, we did not find a different effect for the HAT inhibitors between astrocytes and U87 glioblastoma cell line. This could be explained by multiple reasons. HAT inhibitors act on specific HAT enzymes, which means that these inhibitors would affect certain lysine residues rather than pan histone acetylation. Those specific lysine residues affected might not drive a major difference in chromatin condensation that could give a differential effect in glioblastoma cells versus the astrocytes. This experiment was done as part of preliminary research for applying for a grant to pursue our hypothesis. When we found that the results were not promising, we moved directly to different experiments, without replicating the results, which is why n=1.

We then tested the effect of two HAT inhibitors: Tip60 inhibitor[120] (TH1834) and KAT6A/B inhibitor (WM-8014)[119]. Here, we changed our goal from only trying to protect the DNA from radiation to also assessing the effect of the different HAT inhibitors on DNA repair. As several HAT inhibitors were shown to sensitize tumor cells to radiation by different mechanisms including inhibition of DNA repair[131,132], we thought to use this to our advantage by sensitizing glioblastoma cells to radiation using HAT inhibition. Therefore, the effect of our inhibitors was assessed at two time points: 20 min and 2 hours. The first time point was to assess the effect of HAT inhibition on DNA protection by chromatin condensation. The second time point was to allow for DNA repair to happen and therefore, assess the effect of HAT inhibition on DNA repair, and the amount of DNA damage induced. However, we did not find an effect for the inhibitors on DNA damage in both cases. This could be for several reasons: 1- The inhibitors that were tested, might not have been effective in glioblastoma. To validate this interpretation, HAT inhibitors could have been tested in other cancers or normal cells. 2- The analysis was done after 24 hours of exposing the

cells to HAT inhibitors. This time might have been longer than the time of the effect of HAT inhibitors. To solve this, HAT inhibitors could have been tested in different time points using antibodies to their respective acetylated histone residues, with the rationale of choosing the optimal time for the inhibitors' effect and using that time for our experiments. In these experiments, we used two inhibitors on two different cell lines. When we did not find promising results, we changed our strategy, and we did not replicate the experiments, n=1.

Since all the inhibitors are active only on specific HATs, they would affect the acetylation of certain lysine residues rather than general histone acetylation. Therefore, we needed a different approach to affect the general acetylation. The answer came from multiple studies on the source of substrate for histone acetylation, acetyl CoA. If we consider the HATs to be the writers of epigenetic modifications, then those writers need the "ink". The substrate (Acetyl CoA) for acetylation is not an endless supply, it requires the activation of certain metabolic pathways to be produced.

Significant evidence from the research of Kathryn E. Wellen and others showed that the acetyl CoA that forms the substrate for histone acetylation comes mainly from glucose metabolism, and that the rate of histone acetylation is linked to the rate of glycolysis[82,133,134]. A very interesting finding was that supplementation of glucose-starved cells with fatty acids failed to rescue histone acetylation, which suggests that only nucleocytoplasmic but not mitochondrial acetyl-CoA is available to participate in histone acetylation. This was the basis of our approach to use glucose concentration in order to control histone acetylation. Our goal was to control DNA repair by controlling glucose metabolism, which would open the door for many metabolic drugs to sensitize glioblastoma cells to radiation by inhibiting DNA repair. A finding from the Wellen lab also supported this notion, as they found that nuclear ATP-citrate lyase (ACLY) is phosphorylated

following DNA damage, which facilitates histone acetylation at double-strand break (DSB) sites, impairing 53BP1 localization and enabling BRCA1 recruitment and DNA repair by homologous recombination[89]. Therefore, the inhibition of ACLY inhibited NHEJ and promoted HDR.

We planned our experiment to test the histone acetylation by western blotting, in addition to testing the DNA repair with γH2AX antibodies, so that we can fully understand whether the glucose concentration changes had an effect. We found that neither histone acetylation nor DNA repair were affected by glucose concentrations.

We hypothesized that the cause for these findings is that glioblastoma might obtain the acetyl CoA needed for histone acetylation through multiple resources, and that glucose deprivation would reprogram the glioblastoma cells to direct the production of acetyl CoA through other carbon sources. There were some studies that explored the notion of metabolic reprogramming for lipids to become a main carbon source for histone acetylation[91]. However, what we found very interesting was the glutamine as a source for acetyl CoA through reductive carboxylation, which produces citrate that can later produce Acetyl CoA through ATP citrate lyase (ACLY)[135]. This sparked our interest because it was shown that under hypoxia conditions, cells rely completely on glutamine reductive metabolism to produce acetyl CoA[136]. In addition, under glucose deprivation conditions, SF188 glioblastoma cells were shown to activate an alternative pathway to deliver glutamine carbon to the tricarboxylic acid cycle, with a large increase in the activity of glutamate dehydrogenase (GDH)[137]. We thought that since glioblastoma cells were under glucose deprivation, and the glioblastoma microenvironment would usually be under hypoxic conditions, the glioblastoma cells might have been reprogrammed to use glutamine as a source for acetyl CoA. source for acetyl CoA. However, glutamine deprivation and glutamine and glucose deprivation

had no effect on histone acetylation either. In our future directions, we plan to confirm these findings.

The use of γH2AX foci quantification for assessing DNA repair might not be reliable. McManus et al. showed that in the absence of DNA damage sources, γH2AX foci are still present in hundreds. A few of these foci resembled the ones that were generated after ionizing radiation, and they probably represent naturally occurring DNA double strand breaks (DSB). However, the other sites do not recruit DSB repair proteins, which indicates they are not related to DNA damage[138]. For this reason, we had to choose limiting factors for our foci counting protocol using Imaris software, which only allows a certain size and intensity to be counted as DSB related γH2AX foci. This method could potentially lead to miscounting the DSBs. Therefore, other methods should be used in future studies for evaluating the number of DSBs.

We therefore resorted to an alternative strategy to differentially affect glioblastoma cells, which is using the ketogenic diet (β-hydroxybutyrate) as an alternative source for energy in normal cells, but not for glioblastoma cells. There are two potential benefits for this strategy: 1- Glioblastoma cells do not metabolize β-hydroxybutyrate efficiently, therefore, using β-hydroxybutyrate in a glucose free media as the energy source, would deprive glioblastoma cells from energy. 2- β-hydroxybutyrate was found to supress colorectal cancer through the surface receptor Hcar2 and activating the transcriptional regulator Hopx, which in turn affects gene expression and supresses cell proliferation[139]. Although glioblastoma cells could not survive solely on β-hydroxybutyrate, without glucose, normal cells couldn't survive using it either. Therefore, we thought it was not an effective strategy. We also tested whether the concentration of β-hydroxybutyrate would affect glioblastoma cell growth, and we did not find a difference between β-hydroxybutyrate in different concentrations and the control samples. This could be due to using lower concentrations of β-

hydroxybutyrate than the effective threshold. Moreover, the mentioned study found β-hydroxybutyrate to be effective in vivo[139], which indicates that β-hydroxybutyrate might need cell-cell signaling in order to exert its effect. Finally, β-hydroxybutyrate might be effective in other cancers but not glioblastoma. We can address these questions in future directions.

Finally, we tested sulforaphane, a natural product that comes from broccoli sprouts and has shown promising anti-cancer effects (See introduction), to explore whether it would be effective in glioblastoma therapy. It was shown previously in our lab that both broccoli sprouts and sulforaphane act as a protective agent in the perinatal setting. Placental insufficiency creates a hypoxic-ischemic (HI) environment in-utero, which results in perinatal brain damage to the fetus. This leads to various neurodevelopmental disabilities, which includes cerebral palsy (CP), autism spectrum disorder, attention deficit hyperactive disorder, and epilepsy[140].

In collaboration with Dr. Jerome Yager, our lab has shown in a cell culture setting that sulforaphane has neuroprotective activity when used in small doses[96]. As a part of my colleagues' projects, for determining the impact of sulforaphane on different brain cell types, neurons, astrocytes, and oligodendroglia were cultured under single cell culture conditions as well as co-cultured in an oxygen-glucose deprivation (OGD) environment, and then the LD50 was determined (LD50: duration of OGD required to ensure a cell death of at least 50%). After determining the LD50 of each cell type exposed to oxygen-glucose deprivation (OGD), each cell culture was cultured with a concentration of SFA from 0 (control) to 200 mm and a dose-response curve was delineated to assess both the effective dose for neuroprotection and a possible toxic dose. My colleagues demonstrated that SFA elicited a cellular protective effect on neurons, astrocytes, and a co-culture of both cells at low doses (2.5 mM) when cultured in an oxygen and glucose deprived (OGD) environment to resemble placental insufficiency[96]. Sulforaphane was

shown to induce this protective effect through releasing the transcription factor Nrf2 from protein Keap1. As a result of this, Nrf2 translocate to the nucleus to transcribe antioxidant response element (ARE), which upregulates the antioxidant enzymes' expression, leading to neutralizing reactive oxygen species (ROS).

As mentioned above, at low doses, sulforaphane showed a protective effect, however, at very high concentration (10-fold), sulforaphane was toxic in both OGD and control cell cultures. Our lab concluded through this work that sulforaphane is a hermetic compound, which has a biphasic dose response. Therefore, at high concentrations, sulforaphane induces a proapoptotic function, and exerts an anti-cancerous activity, while at low concentrations, it is antiapoptotic and cell protective. This indicates that there might be a change in mechanism between high and low doses of sulforaphane.

This paradoxical response sparked my interest in exploring sulforaphane as anti-cancer agent for glioblastoma, which would lead to exerting anti-cancer activity, while protecting the normal tissues. Other researchers found that the mechanisms by which sulforaphane was found to elicit an anti-cancer activity were various, and not limited to a certain pathway. These pathways included: (1) the generation of reactive oxygen species (ROS) in cancer cells, which induces an intracellular toxic environment, leading to apoptosis. (2) Increasing the expression of death receptors, which leads to signalling apoptosis through the extrinsic pathway. (3) Inhibition of HDAC enzymes, which leads to silencing oncogenes and activating tumor-suppressor genes, leading to apoptosis and cell cycle arrest in tumor cells. (4) Inhibition of cancer stem cell formation. (5) Activation of the endoplasmic reticulum (ER) stress. The activation of apoptosis through multiple pathways made sulforaphane effective for multiple cancers, with low potential for resistance (see introduction for references).

In this study, we have shown that sulforaphane exerted a cytotoxic effect in a dose-dependent manner, with a relatively low LD50. We also showed that sulforaphane inhibited cell cycle progression, which is very essential for controlling tumor growth. We demonstrated an anti-invasive effect for sulforaphane in U87 cell line at very low doses. U251 are not invasive in vitro, therefore we didn't use them for this assay.

The combination of sulforaphane with radiation was demonstrated in different studies to greatly enhance the efficacy of radiation. For example, sulforaphane in combination with radiation was demonstrated to induce strong and dose dependent survival reduction in clonogenic assays, an induction of a G2/M cell cycle arrest and an increase in γH2AX phosphorylation level indicating DNA damage, In four established pancreatic cancer cell line[141].

However, to our knowledge, the combination of sulforaphane and radiation wasn't studies in glioblastoma before. We found sulforaphane to be a promising agent due to its cytotoxic along with anti-invasion activity on glioblastoma cell lines. In addition, we have combined sulforaphane with radiation for cytotoxic analysis, and we showed that sulforaphane had significant cytotoxic effect. However, the effect was not potentiated by radiation in this experiment. The reason for this is that metabolic assays are not effective in showing the effects of radiation. We are currently performing a colony-forming assay to assess the effect of this combination on colony forming properties of glioblastoma.

CHAPTER 5: Conclusions and future directions

5.0 Conclusions and future directions

This study explored four different approaches to impact glioblastoma therapy. For the first approach, we explored the possibility of using a HAT inhibitor, to selectively increase the sensitivity of glioblastoma cells to radiation. However, we did not find a significant effect of HAT inhibition on glioblastoma sensitivity to radiation.

In the second approach in our study, we changed the HAT inhibition strategy to impacting the histone acetylation directly without HAT inhibition. We did that through affecting the substrate for acetylation "Acetyl CoA", which is produced in the cell through glucose. We explored the effect of changing the glucose concentration on the histone acetylation. We did not find any effect of the glucose concentrations on the histone acetylation. We also researched the effect of changing the glucose concentration on radiation mediated DNA damage, and we did not find an effect. For future studies, other metabolic sources such as fat and glutamine should be explored as an alternative source for histone acetylation substrate. In addition, a comparison study should be made between different cancers using different sources for acetyl CoA for histone acetylation. Moreover, if the source for histone acetylation was found in glioblastoma, we will investigate the effect of changing the levels of this metabolic source on DNA repair as well.

In our third approach we used ketogenic diet as an alternative energy source to glucose for our cultured cells. The rationale for this approach was that glioblastoma cells lack the enzyme for metabolizing β-Hydroxybutyrate, while normal cells don't. Therefore, using the ketogenic diet could induce a selective energy deprivation for the glioblastoma cells. We found that glioblastoma cells couldn't survive using ketogenic diet. However, normal astrocytes weren't able to metabolize β-Hydroxybutyrate either. In future directions, ketogenic diet could be explored in preclinical animal models.

Finally, we explored the anti-cancer properties of sulforaphane on glioblastoma cells. We found that sulforaphane had cytotoxic effects on glioblastoma cells, as indicated by alamarBlue metabolic assay. In addition, sulforaphane inhibited the invasion of U251 and U87 glioblastoma cell lines in culture. Moreover, sulforaphane induced cell cycle arrest for U251 cells. Finally, we tested the synergy between sulforaphane and radiation. Using alamarBlue survival assay, we did not find a synergy between sulforaphane and radiation.

For future directions, we plan to do a clonogenic assay to test the synergy between sulforaphane and radiation. Furthermore, we will test the mechanism of sulforaphane action as an HDAC inhibitor in glioblastoma. In addition, we will explore the effect of sulforaphane on apoptotic protein expression, such as Caspase 3 and Bax/BCL2 ratio. Finally, we will test sulforaphane in glioblastoma animal models.

Bibliography

1. Schwartzbaum, J. A., Fisher, J. L., Aldape, K. D. & Wrensch, M. Epidemiology and molecular pathology of glioma. *Nature Clinical Practice Neurology* (2006) doi:10.1038/ncpneuro0289.

2. Ichimura, K., Ohgaki, H., Kleihues, P. & Collins, V. P. Molecular pathogenesis of astrocytic tumours. *Journal of Neuro-Oncology* (2004) doi:10.1007/s11060-004-2747-2.

3. Thakkar, J. P. *et al.* Epidemiologic and molecular prognostic review of glioblastoma. *Cancer Epidemiology Biomarkers and Prevention* (2014) doi:10.1158/1055-9965.EPI-14-0275.

4. Taylor, O. G., Brzozowski, J. S. & Skelding, K. A. Glioblastoma multiforme: An overview of emerging therapeutic targets. *Frontiers in Oncology* (2019) doi:10.3389/fonc.2019.00963.

5. Davis, M. E. Glioblastoma: Overview of disease and treatment. *Clin. J. Oncol. Nurs.* (2016) doi:10.1188/16.CJON.S1.2-8.

6. Stupp, R. *et al.* Radiotherapy plus Concomitant and Adjuvant Temozolomide for Glioblastoma. *N. Engl. J. Med.* (2005) doi:10.1056/nejmoa043330.

7. Lee, S. Y. Temozolomide resistance in glioblastoma multiforme. *Genes and Diseases* (2016) doi:10.1016/j.gendis.2016.04.007.

8. Stewart, L. A. Chemotherapy in adult high-grade glioma: A systematic review and meta-analysis of individual patient data from 12 randomised trials. *Lancet* (2002) doi:10.1016/S0140-6736(02)08091-1.

9. Malmer, B., Grönberg, H., Bergenheim, A. T., Lenner, P. & Henriksson, R. Familial aggregation of astrocytoma in Northern Sweden: An epidemiological cohort study. *Int. J. Cancer* (1999) doi:10.1002/(SICI)1097-0215(19990505)81:3<366::AID-IJC9>3.0.CO;2-0.

10. O'Neill, B. P. *et al.* Risk of cancer among relatives of patients with glioma. *Cancer Epidemiol. Biomarkers Prev.* (2002).

11. Blowers, L., Preston-Martin, S. & Mack, W. J. Dietary and other lifestyle factors of women with brain gliomas in Los Angeles County (California, USA). *Cancer Causes Control* (1997) doi:10.1023/A:1018437031987.

12. Lee, M., Wrensch, M. & Miike, R. Dietary and tobacco risk factors for adult onset glioma in the San Francisco Bay Area (California, USA). *Cancer Causes Control* (1997) doi:10.1023/A:1018470802969.

13. Boeing, H., Schlehofer, B., Blettner, M. & Wahrendorf, J. Dietary carcinogens and the risk for glioma and meningioma in Germany. *Int. J. Cancer* (1993) doi:10.1002/ijc.2910530406.

14. Edick, M. J. *et al.* Lymphoid gene expression as a predictor of risk of secondary brain tumors. *Genes Chromosom. Cancer* (2005) doi:10.1002/gcc.20121.

15. Ohgaki, H. *et al.* Genetic pathways to glioblastoma: A population-based study. *Cancer Res.* (2004) doi:10.1158/0008-5472.CAN-04-1337.

16. Kaminska, B., Czapski, B., Guzik, R., Król, S. K. & Gielniewski, B. Consequences of IDH1/2 mutations in gliomas and an assessment of inhibitors targeting mutated IDH proteins. *Molecules*

(2019) doi:10.3390/molecules24050968.

17. McLendon, R. *et al.* Comprehensive genomic characterization defines human glioblastoma genes and core pathways. *Nature* (2008) doi:10.1038/nature07385.

18. Nishikawa, R. *et al.* A mutant epidermal growth factor receptor common in human glioma confers enhanced tumorigenicity. *Proc. Natl. Acad. Sci. U. S. A.* (1994) doi:10.1073/pnas.91.16.7727.

19. Kato, S. *et al.* Revisiting Epidermal Growth Factor Receptor (EGFR) Amplification as a Target for Anti-EGFR Therapy: Analysis of Cell-Free Circulating Tumor DNA in Patients With Advanced Malignancies . *JCO Precis. Oncol.* (2019) doi:10.1200/po.18.00180.

20. Ichimura, K., Schmidt, E. E., Goike, H. M. & Collins, V. P. Human glioblastomas with no alterations of the CDKN2A (p16(INK4A), MTS1) and CDK4 genes have frequent mutations of the retinoblastoma gene. *Oncogene* (1996).

21. Ichimura, K. *et al.* Deregulation of the p14(ARF)/MDM2/p53 pathway is a prerequisite for human astrocytic gliomas with G1-S transition control gene abnormalities. *Cancer Res.* (2000).

22. Cobbs, C. S. *et al.* Inactivation of Wild-Type p53 Protein Function by Reactive Oxygen and Nitrogen Species in Malignant Glioma Cells. *Cancer Res.* (2003).

23. Ehrlich, M. DNA methylation in cancer: Too much, but also too little. *Oncogene* (2002) doi:10.1038/sj.onc.1205651.

24. Gaudet, F. *et al.* Induction of tumors in mice by genomic hypomethylation. *Science (80-.).* (2003) doi:10.1126/science.1083558.

25. Schulz, W. A. *et al.* Genomewide DNA hypomethylation is associated with alterations on chromosome 8 in prostate carcinoma. *Genes Chromosom. Cancer* (2002) doi:10.1002/gcc.10092.

26. Eden, A., Gaudet, F., Waghmare, A. & Jaenisch, R. Chromosomal instability and tumors promoted by DNA hypomethylation. *Science* (2003) doi:10.1126/science.1083557.

27. Howard, G., Eiges, R., Gaudet, F., Jaenisch, R. & Eden, A. Activation and transposition of endogenous retroviral elements in hypomethylation induced tumors in mice. *Oncogene* (2008) doi:10.1038/sj.onc.1210631.

28. Kan, S., Chai, S., Chen, W. & Yu, B. DNA methylation profiling identifies potentially significant epigenetically-regulated genes in glioblastoma multiforme. *Oncol. Lett.* (2019) doi:10.3892/ol.2019.10512.

29. Cadieux, B., Ching, T. T., VandenBerg, S. R. & Costello, J. F. Genome-wide hypomethylation in human glioblastomas associated with specific copy number alteration, methylenetetrahydrofolate reductase allele status, and increased proliferation. *Cancer Res.* (2006) doi:10.1158/0008-5472.CAN-06-1547.

30. Feinberg, A. P. & Tycko, B. The history of cancer epigenetics. *Nature Reviews Cancer* (2004) doi:10.1038/nrc1279.

31. Amatya, V. J., Naumann, U., Weller, M. & Ohgaki, H. TP53 promoter methylation in human gliomas. *Acta Neuropathol.* (2005) doi:10.1007/s00401-005-1041-5.

32. Nakamura, M., Yonekawa, Y., Kleihues, P. & Ohgaki, H. Promoter hypermethylation of the RB1 gene in glioblastomas. *Lab. Investig.* (2001) doi:10.1038/labinvest.3780213.

33. Baeza, N., Weller, M., Yonekawa, Y., Kleihues, P. & Ohgaki, H. PTEN methylation and expression in glioblastomas. *Acta Neuropathol.* (2003) doi:10.1007/s00401-003-0748-4.

34. Waha, A. *et al.* Epigenetic silencing of the protocadherin family member PCDH-γ-A11 in astrocytomas. *Neoplasia* (2005) doi:10.1593/neo.04490.

35. Zhou, H. *et al.* Reciprocal regulation of SOCS1 and SOCS3 enhances resistance to ionizing radiation in glioblastoma multiforme. *Clin. Cancer Res.* (2007) doi:10.1158/1078-0432.CCR-06-2303.

36. Gerson, S. L. MGMT: Its role in cancer aetiology and cancer therapeutics. *Nature Reviews Cancer* (2004) doi:10.1038/nrc1319.

37. Wick, W. *et al.* MGMT testing - The challenges for biomarker-based glioma treatment. *Nature Reviews Neurology* (2014) doi:10.1038/nrneurol.2014.100.

38. Sidaway, P. CNS cancer: Glioblastoma subtypes revisited. *Nature Reviews Clinical Oncology* (2017) doi:10.1038/nrclinonc.2017.122.

39. Capper, D. *et al.* DNA methylation-based classification of central nervous system tumours. *Nature* (2018) doi:10.1038/nature26000.

40. Ma, H. *et al.* Specific glioblastoma multiforme prognostic-subtype distinctions based on DNA methylation patterns. *Cancer Gene Ther.* (2019) doi:10.1038/s41417-019-0142-6.

41. Zheng, S. *et al.* DNA hypermethylation profiles associated with glioma subtypes and EZH2 and IGFBP2 mRNA expression. *Neuro. Oncol.* (2011) doi:10.1093/neuonc/noq190.

42. Kim, Y. Z. Altered Histone Modifications in Gliomas. *Brain Tumor Res. Treat.* (2014) doi:10.14791/btrt.2014.2.1.7.

43. Ferreira, W. A. S. *et al.* An update on the epigenetics of glioblastomas. *Epigenomics* (2016) doi:10.2217/epi-2016-0040.

44. Zentner, G. E. & Henikoff, S. Regulation of nucleosome dynamics by histone modifications. *Nature Structural and Molecular Biology* (2013) doi:10.1038/nsmb.2470.

45. Fraga, M. F. *et al.* Loss of acetylation at Lys16 and trimethylation at Lys20 of histone H4 is a common hallmark of human cancer. *Nat. Genet.* (2005) doi:10.1038/ng1531.

46. Lucio-Eterovic, A. K. B. *et al.* Differential expression of 12 histone deacetylase (HDAC) genes in astrocytomas and normal brain tissue: Class II and IV are hypoexpressed in glioblastomas. *BMC Cancer* (2008) doi:10.1186/1471-2407-8-243.

47. Wu, G. *et al.* Somatic histone H3 alterations in pediatric diffuse intrinsic pontine gliomas and non-brainstem glioblastomas. *Nat. Genet.* (2012) doi:10.1038/ng.1102.

48. Wu, G. *et al.* The genomic landscape of diffuse intrinsic pontine glioma and pediatric non-brainstem high-grade glioma. *Nat. Genet.* (2014) doi:10.1038/ng.2938.

49. Schwartzentruber, J. *et al.* Driver mutations in histone H3.3 and chromatin remodelling genes in

paediatric glioblastoma. *Nature* (2012) doi:10.1038/nature10833.

50. Das, K. K. *et al.* Pediatric glioblastoma: Clinico-radiological profile and factors affecting the outcome. *Child's Nerv. Syst.* (2012) doi:10.1007/s00381-012-1890-x.

51. Pollack, I. F. *et al.* IDH1 mutations are common in malignant gliomas arising in adolescents: A report from the Children's Oncology Group. *Child's Nerv. Syst.* (2011) doi:10.1007/s00381-010-1264-1.

52. Narayana, A. *et al.* Bevacizumab in recurrent high-grade pediatric gliomas. *Neuro. Oncol.* (2010) doi:10.1093/neuonc/noq033.

53. Artico, M., Cervoni, L., Celli, P., Salvati, M. & Palma, L. Supratentorial glioblastoma in children: a series of 27 surgically treated cases. *Child's Nerv. Syst.* (1993) doi:10.1007/BF00301926.

54. Ali, M. Y. *et al.* Radioresistance in glioblastoma and the development of radiosensitizers. *Cancers* (2020) doi:10.3390/cancers12092511.

55. Tang, L., Feng, Y., Gao, S., Mu, Q. & Liu, C. Nanotherapeutics Overcoming the Blood-Brain Barrier for Glioblastoma Treatment. *Frontiers in Pharmacology* (2021) doi:10.3389/fphar.2021.786700.

56. Lim, M., Xia, Y., Bettegowda, C. & Weller, M. Current state of immunotherapy for glioblastoma. *Nature Reviews Clinical Oncology* (2018) doi:10.1038/s41571-018-0003-5.

57. Shergalis, A., Bankhead, A., Luesakul, U., Muangsin, N. & Neamati, N. Current challenges and opportunities in treating glioblastomas. *Pharmacol. Rev.* (2018) doi:10.1124/pr.117.014944.

58. Komotar, R. J., Otten, M. L., Moise, G. & Connolly, E. S. Radiotherapy plus concomitant and adjuvant temozolomide for glioblastoma—A critical review. *Clinical Medicine: Oncology* (2008) doi:10.4137/cmo.s390.

59. Lawson, H. C. *et al.* Interstitial chemotherapy for malignant gliomas: The Johns Hopkins experience. *J. Neurooncol.* (2007) doi:10.1007/s11060-006-9303-1.

60. Hatoum, A., Mohammed, R. & Zakieh, O. The unique invasiveness of glioblastoma and possible drug targets on extracellular matrix. *Cancer Management and Research* (2019) doi:10.2147/CMAR.S186142.

61. Duan, Q., Zhang, H., Zheng, J. & Zhang, L. Turning Cold into Hot: Firing up the Tumor Microenvironment. *Trends in Cancer* (2020) doi:10.1016/j.trecan.2020.02.022.

62. Radford, I. R. The level of induced DNA double-Strand breakage correlates with cell killing after x-irradiation. *Int. J. Radiat. Biol.* (1985) doi:10.1080/09553008514551051.

63. Jorgensen, T. J. Enhancing radiosensitivity: Targeting the DNA repair pathways. *Cancer Biology and Therapy* (2009) doi:10.4161/cbt.8.8.8304.

64. Misteli, T. & Soutoglou, E. The emerging role of nuclear architecture in DNA repair and genome maintenance. *Nature Reviews Molecular Cell Biology* (2009) doi:10.1038/nrm2651.

65. Dhar, S., Gursoy-Yuzugullu, O., Parasuram, R. & Price, B. D. The tale of a tail: Histone H4 acetylation and the repair of DNA breaks. *Philosophical Transactions of the Royal Society B: Biological Sciences* (2017) doi:10.1098/rstb.2016.0284.

66. Ceccaldi, R., Rondinelli, B. & D'Andrea, A. D. Repair Pathway Choices and Consequences at the Double-Strand Break. *Trends in Cell Biology* (2016) doi:10.1016/j.tcb.2015.07.009.

67. Shiloh, Y. & Ziv, Y. The ATM protein kinase: Regulating the cellular response to genotoxic stress, and more. *Nature Reviews Molecular Cell Biology* (2013) doi:10.1038/nrm3546.

68. Stucki, M. *et al.* MDC1 directly binds phosphorylated histone H2AX to regulate cellular responses to DNA double-strand breaks. *Cell* (2005) doi:10.1016/j.cell.2005.09.038.

69. Ramachandran, S. *et al.* The RNF8/RNF168 ubiquitin ligase cascade facilitates class switch recombination. *Proc. Natl. Acad. Sci. U. S. A.* (2010) doi:10.1073/pnas.0913790107.

70. Fradet-Turcotte, A. *et al.* 53BP1 is a reader of the DNA-damage-induced H2A Lys 15 ubiquitin mark. *Nature* (2013) doi:10.1038/nature12318.

71. Lai, W. K. M. & Pugh, B. F. Understanding nucleosome dynamics and their links to gene expression and DNA replication. *Nature Reviews Molecular Cell Biology* (2017) doi:10.1038/nrm.2017.47.

72. Cutter, A. R. & Hayes, J. J. A brief review of nucleosome structure. *FEBS Letters* (2015) doi:10.1016/j.febslet.2015.05.016.

73. Gong, F., Chiu, L. Y. & Miller, K. M. Acetylation Reader Proteins: Linking Acetylation Signaling to Genome Maintenance and Cancer. *PLoS Genetics* (2016) doi:10.1371/journal.pgen.1006272.

74. Bannister, A. J. & Kouzarides, T. Regulation of chromatin by histone modifications. *Cell Research* (2011) doi:10.1038/cr.2011.22.

75. Shahbazian, M. D. & Grunstein, M. Functions of Site-Specific histone acetylation and deacetylation. *Annual Review of Biochemistry* (2007) doi:10.1146/annurev.biochem.76.052705.162114.

76. Shogren-Knaak, M. *et al.* Histone H4-K16 acetylation controls chromatin structure and protein interactions. *Science (80-.).* (2006) doi:10.1126/science.1124000.

77. Kalashnikova, A. A., Porter-Goff, M. E., Muthurajan, U. M., Luger, K. & Hansen, J. C. The role of the nucleosome acidic patch in modulating higher order chromatin structure. *Journal of the Royal Society Interface* (2013) doi:10.1098/rsif.2012.1022.

78. Jacquet, K. *et al.* The TIP60 Complex Regulates Bivalent Chromatin Recognition by 53BP1 through Direct H4K20me Binding and H2AK15 Acetylation. *Mol. Cell* (2016) doi:10.1016/j.molcel.2016.03.031.

79. Tang, J. *et al.* Acetylation limits 53BP1 association with damaged chromatin to promote homologous recombination. *Nat. Struct. Mol. Biol.* (2013) doi:10.1038/nsmb.2499.

80. Chiu, L. Y., Gong, F. & Miller, K. M. Bromodomain proteins: Repairing DNA damage within chromatin. *Philosophical Transactions of the Royal Society B: Biological Sciences* (2017) doi:10.1098/rstb.2016.0286.

81. Wellen, K. E. *et al.* ATP-citrate lyase links cellular metabolism to histone acetylation. *Science (80-.).* (2009) doi:10.1126/science.1164097.

82. Lee, J. V. *et al.* Akt-dependent metabolic reprogramming regulates tumor cell Histone

acetylation. *Cell Metab.* (2014) doi:10.1016/j.cmet.2014.06.004.

83. Zhao, S. *et al.* ATP-Citrate Lyase Controls a Glucose-to-Acetate Metabolic Switch. *Cell Rep.* (2016) doi:10.1016/j.celrep.2016.09.069.

84. Campbell, S. L. & Wellen, K. E. Metabolic Signaling to the Nucleus in Cancer. *Molecular Cell* (2018) doi:10.1016/j.molcel.2018.07.015.

85. Cluntun, A. A. *et al.* The rate of glycolysis quantitatively mediates specific histone acetylation sites. *Cancer Metab.* (2015) doi:10.1186/s40170-015-0135-3.

86. Sivanand, S., Viney, I. & Wellen, K. E. Spatiotemporal Control of Acetyl-CoA Metabolism in Chromatin Regulation. *Trends in Biochemical Sciences* (2018) doi:10.1016/j.tibs.2017.11.004.

87. Evertts, A. G. *et al.* Quantitative dynamics of the link between cellular metabolism and histone acetylation. *J. Biol. Chem.* (2013) doi:10.1074/jbc.M112.428318.

88. Liu, J. Y. & Wellen, K. E. Advances into understanding metabolites as signaling molecules in cancer progression. *Current Opinion in Cell Biology* (2020) doi:10.1016/j.ceb.2020.01.013.

89. Sivanand, S. *et al.* Nuclear Acetyl-CoA Production by ACLY Promotes Homologous Recombination. *Mol. Cell* (2017) doi:10.1016/j.molcel.2017.06.008.

90. Ampferl, R., Rodemann, H. P., Mayer, C., Höfling, T. T. A. & Dittmann, K. Glucose starvation impairs DNA repair in tumour cells selectively by blocking histone acetylation. *Radiother. Oncol.* (2018) doi:10.1016/j.radonc.2017.10.020.

91. McDonnell, E. *et al.* Lipids Reprogram Metabolism to Become a Major Carbon Source for Histone Acetylation. *Cell Rep.* (2016) doi:10.1016/j.celrep.2016.10.012.

92. Klein, P., Tyrlikova, I., Zuccoli, G., Tyrlik, A. & Maroon, J. C. Treatment of glioblastoma multiforme with “classic” 4:1 ketogenic diet total meal replacement. *Cancer Metab.* (2020) doi:10.1186/s40170-020-00230-9.

93. Maurer, G. D. *et al.* Differential utilization of ketone bodies by neurons and glioma cell lines: A rationale for ketogenic diet as experimental glioma therapy. *BMC Cancer* (2011) doi:10.1186/1471-2407-11-315.

94. Li, J., Zhang, H. & Dai, Z. Cancer Treatment With the Ketogenic Diet: A Systematic Review and Meta-analysis of Animal Studies. *Front. Nutr.* (2021) doi:10.3389/fnut.2021.594408.

95. Woolf, E. C., Syed, N. & Scheck, A. C. Tumor metabolism, the ketogenic diet and β-hydroxybutyrate: Novel approaches to adjuvant brain tumor therapy. *Front. Mol. Neurosci.* (2016) doi:10.3389/fnmol.2016.00122.

96. Ladak, Z. *et al.* Sulforaphane (SFA) protects neuronal cells from oxygen & glucose deprivation (OGD). *PLoS One* (2021) doi:10.1371/journal.pone.0248777.

97. Fahey, J. W. *et al.* Sulforaphane bioavailability from glucoraphanin-rich broccoli: Control by active endogenous myrosinase. *PLoS One* (2015) doi:10.1371/journal.pone.0140963.

98. Klomparens, E. & Ding, Y. The neuroprotective mechanisms and effects of sulforaphane. *Brain Circ.* (2019) doi:10.4103/bc.bc_7_19.

99. Ladak, Z., Khairy, M., Armstrong, E. A. & Yager, J. Y. Chapter 11 - Glucosinolates: paradoxically beneficial in fighting both brain cell death and cancer. in *Nutraceuticals in Brain Health and Beyond* (2021).

100. Liou, G. Y. & Storz, P. Reactive oxygen species in cancer. *Free Radical Research* (2010) doi:10.3109/10715761003667554.

101. Cho, J., Kim, Y., Young, B. & Keum, Y. Sulforaphane inhibition of TPA-mediated PDCD4 downregulation contributes to suppression of c-Jun and induction of p21-dependent Nrf2 expression. *Eur. J. Pharmacol.* **741**, 247–253 (2014).

102. Lan, H., Yuan, H. & Lin, C. Sulforaphane induces p53-deficient SW480 cell apoptosis via the ROS-MAPK signaling pathway. *Mol. Med. Rep.* **16**, 7796–7804 (2017).

103. Flavahan, W. A., Gaskell, E. & Bernstein, B. E. Epigenetic plasticity and the hallmarks of cancer. *Science* (2017) doi:10.1126/science.aal2380.

104. Li, Y. & Seto, E. HDACs and HDAC inhibitors in cancer development and therapy. *Cold Spring Harb. Perspect. Med.* (2016) doi:10.1101/cshperspect.a026831.

105. Myzak, M. C., Karplus, P. A., Chung, F. L. & Dashwood, R. H. A novel mechanism of chemoprotection by sulforaphane: Inhibition of histone deacetylase. *Cancer Res.* (2004) doi:10.1158/0008-5472.CAN-04-1326.

106. Ho, E., Clarke, J. D. & Dashwood, R. H. Dietary sulforaphane, a histone deacetylase inhibitor for cancer prevention. in *Journal of Nutrition* (2009). doi:10.3945/jn.109.113332.

107. Yang, F. *et al.* Sulforaphane induces autophagy by inhibition of HDAC6-mediated PTEN activation in triple negative breast cancer cells. *Life Sci.* **213**, 149–157 (2018).

108. Zhou, J. *et al.* nAChRs-ERK1/2-Egr-1 signaling participates in the developmental toxicity of nicotine by epigenetically down-regulating placental 11β-HSD2. *Toxicology and Applied Pharmacology* (2018) doi:10.1016/j.taap.2018.02.017.

109. Geng, Y. *et al.* Sulforaphane induced apoptosis via promotion of mitochondrial fusion and ERK1/2-mediated 26s proteasome degradation of novel pro-survival bim and upregulation of bax in human non-small cell lung cancer cells. *J. Cancer* **8**, 2456–2470 (2017).

110. Kan, S. F., Wang, J. & Sun, G. X. Sulforaphane regulates apoptosis- and proliferation-related signaling pathways and synergizes with cisplatin to suppress human Ovarian cancer. *Int. J. Mol. Med.* **42**, 2447–2458 (2018).

111. Lewinska, A., Adamczyk-Grochala, J., Deregowska, A. & Wnuk, M. Sulforaphane-induced cell cycle arrest and senescence are accompanied by DNA hypomethylation and changes in microRNA profile in breast cancer cells. *Theranostics* **7**, 3461–3477 (2017).

112. Zhou, L. *et al.* Sulforaphane-induced apoptosis in Xuanwei lung adenocarcinoma cell line XWLC-05. *Thorac. Cancer* **8**, 16–25 (2017).

113. Liu, H.-J. *et al.* Sulforaphane-N-Acetyl-Cysteine Induces Autophagy Through Activation of ERK1/2 in U87MG and U373MG Cells. *Cell. Physiol. Biochem.* **51**, 528–542 (2018).

114. Li, C. *et al.* Sulforaphane inhibits invasion via activating ERK1/2 signaling in human glioblastoma

U87MG and U373MG cells. *PLoS One* (2014) doi:10.1371/journal.pone.0090520.

115. Bijangi-Vishehsaraei, K. *et al.* Sulforaphane suppresses the growth of glioblastoma cells, glioblastoma stem cell–like spheroids, and tumor xenografts through multiple cell signaling pathways. *J. Neurosurg.* (2017) doi:10.3171/2016.8.JNS161197.

116. Lan, F., Pan, Q., Yu, H. & Yue, X. Sulforaphane enhances temozolomide-induced apoptosis because of down-regulation of miR-21 via Wnt/β-catenin signaling in glioblastoma. *J. Neurochem.* (2015) doi:10.1111/jnc.13174.

117. Ali, N. *et al.* Osteosarcoma progression is associated with increased nuclear levels and transcriptional activity of activated β-catenin. *Genes and Cancer* (2019) doi:10.18632/oncoscience.191.

118. Garcia, E. *et al.* Inhibition of triple negative breast cancer metastasis and invasiveness by novel drugs that target epithelial to mesenchymal transition. *Sci. Rep.* (2021) doi:10.1038/s41598-021-91344-7.

119. Baell, J. B. *et al.* Inhibitors of histone acetyltransferases KAT6A/B induce senescence and arrest tumour growth. *Nature* (2018) doi:10.1038/s41586-018-0387-5.

120. Gao, C. *et al.* Rational design and validation of a Tip60 histone acetyltransferase inhibitor. *Sci. Rep.* (2014) doi:10.1038/srep05372.

121. Kendall, R. T. & Feghali-Bostwick, C. A. Fibroblasts in fibrosis: Novel roles and mediators. *Frontiers in Pharmacology* (2014) doi:10.3389/fphar.2014.00123.

122. de Ridder, L. I., Laerum, O. D., Mørk, S. J. & Bigner, D. D. Invasiveness of human glioma cell lines in vitro: Relation to tumorigenicity in athymic mice. *Acta Neuropathol.* (1987) doi:10.1007/BF00691091.

123. Myzak, M. C., Karplus, P. A., Chung, F. L. & Dashwood, R. H. A novel mechanism of chemoprotection by sulforaphane: Inhibition of histone deacetylase. *Cancer Res.* (2004) doi:10.1158/0008-5472.CAN-04-1326.

124. Karagiannis, T. C. & El-Osta, A. Modulation of cellular radiation responses by histone deacetylase inhibitors. *Oncogene* (2006) doi:10.1038/sj.onc.1209417.

125. Makale, M. T., McDonald, C. R., Hattangadi-Gluth, J. A. & Kesari, S. Mechanisms of radiotherapy-associated cognitive disability in patients with brain tumours. *Nature Reviews Neurology* (2016) doi:10.1038/nrneurol.2016.185.

126. Dropcho, E. J. Neurotoxicity of Radiation Therapy. *Neurologic Clinics* (2010) doi:10.1016/j.ncl.2009.09.008.

127. Ruben, J. D. *et al.* Cerebral radiation necrosis: Incidence, outcomes, and risk factors with emphasis on radiation parameters and chemotherapy. *Int. J. Radiat. Oncol. Biol. Phys.* (2006) doi:10.1016/j.ijrobp.2005.12.002.

128. Svetličič, M. *et al.* Alpha Radiation as a Way to Target Heterochromatic and Gamma Radiation-Exposed Breast Cancer Cells. *Cells* (2020) doi:10.3390/cells9051165.

129. Falk, M., Lukášová, E. & Kozubek, S. Chromatin structure influences the sensitivity of DNA to γ-

radiation. *Biochim. Biophys. Acta - Mol. Cell Res.* (2008) doi:10.1016/j.bbamcr.2008.07.010.

130. Ehrenhofer-Murray, A. E. Chromatin dynamics at DNA replication, transcription and repair. *European Journal of Biochemistry* (2004) doi:10.1111/j.1432-1033.2004.04162.x.

131. Sun, Y., Jiang, X., Chen, S. & Price, B. D. Inhibition of histone acetyltransferase activity by anacardic acid sensitizes tumor cells to ionizing radiation. *FEBS Lett.* (2006) doi:10.1016/j.febslet.2006.06.092.

132. Oike, T. *et al.* C646, a selective small molecule inhibitor of histone acetyltransferase p300, radiosensitizes lung cancer cells by enhancing mitotic catastrophe. *Radiother. Oncol.* (2014) doi:10.1016/j.radonc.2014.03.015.

133. Wellen, K. E. *et al.* ATP-citrate lyase links cellular metabolism to histone acetylation. *Science (80-.).* (2009) doi:10.1126/science.1164097.

134. Kinnaird, A., Zhao, S., Wellen, K. E. & Michelakis, E. D. Metabolic control of epigenetics in cancer. *Nature Reviews Cancer* (2016) doi:10.1038/nrc.2016.82.

135. Feron, O. The many metabolic sources of acetyl-CoA to support histone acetylation and influence cancer progression. *Ann. Transl. Med.* (2019) doi:10.21037/atm.2019.11.140.

136. Metallo, C. M. *et al.* Reductive glutamine metabolism by IDH1 mediates lipogenesis under hypoxia. *Nature* (2012) doi:10.1038/nature10602.

137. Chendong, Y. *et al.* Glioblastoma cells require glutamate dehydrogenase to survive impairments of glucose metabolism or Akt signaling. *Cancer Res.* (2009) doi:10.1158/0008-5472.CAN-09-2266.

138. McManus, K. J. & Hendzel, M. J. ATM-dependent DNA damage-independent mitotic phosphorylation of H2AX in normally growing mammalian cells. *Mol. Biol. Cell* (2005) doi:10.1091/mbc.E05-01-0065.

139. Dmitrieva-Posocco, O. *et al.* β-Hydroxybutyrate suppresses colorectal cancer. *Nat. 2022 6057908* **605**, 160–165 (2022).

140. *Nutraceuticals in Brain Health and Beyond*. *Nutraceuticals in Brain Health and Beyond* (2021). doi:10.1016/c2018-0-05578-4.

141. Naumann, P. *et al.* Sulforaphane enhances irradiation effects in terms of perturbed cell cycle progression and increased DNA damage in pancreatic cancer cells. *PLoS One* (2017) doi:10.1371/journal.pone.0180940.